

8-2006

Electrorheology of fullerene suspensions

Maricela Lizcano
University of Texas-Pan American

Follow this and additional works at: https://scholarworks.utrgv.edu/leg_etd



Part of the [Mechanical Engineering Commons](#)

Recommended Citation

Lizcano, Maricela, "Electrorheology of fullerene suspensions" (2006). *Theses and Dissertations - UTB/UTPA*. 763.

https://scholarworks.utrgv.edu/leg_etd/763

This Thesis is brought to you for free and open access by ScholarWorks @ UTRGV. It has been accepted for inclusion in Theses and Dissertations - UTB/UTPA by an authorized administrator of ScholarWorks @ UTRGV. For more information, please contact justin.white@utrgv.edu, william.flores01@utrgv.edu.

ELECTRORHEOLOGY OF C₆₀ SUSPENSIONS

A Thesis

by

MARICELA LIZCANO

**Submitted to the Graduate School of the
University of Texas-Pan American
In partial fulfillment of the requirements for the degree of**

MASTER OF SCIENCE

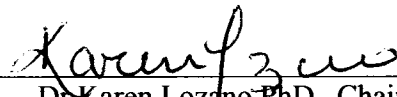
August 2006

Major Subject: Mechanical Engineering

ELECTRORHEOLOGY OF C₆₀ SUSPENSIONS

A Thesis
by
MARICELA LIZCANO

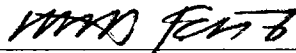
Approved as to style and content by:



Dr. Karen Lozano PhD., Chair
Associate Professor
University of Texas Pan American



Dr. Hashim Madhi PhD.
Chair of the Mechanical Engineering Department
University of Texas Pan American



Dr. Heinrich Foltz PhD.
Chair of the Electrical Engineering Department
University of Texas Pan American

August 2006

ABSTRACT

Lizcano, Maricela., Electrorheology of C₆₀ Suspensions. Master of Science (MS), August, 2006, 88 pp., 3 tables, 46 illustrations, references, 63 titles.

Electrorheological fluids are suspension materials whose rheological behavior changes with an applied voltage. In particular, the material changes from a fluid to a solid behavior with an applied voltage and reverses to its original state when the voltage is removed. This function classifies ER fluids as smart materials. ER fluids may be developed and used as mechanical devices with no mechanical parts such as pumps, actuators, and dampers. Until recently, research was concentrated with micro-particle suspension fluids. This research project investigates the electrorheology of carbon nano-particle suspension.

ACKNOWLEDGEMENTS

This project was funded by the National Science Foundation Bridge to the Doctorate Program. The author wishes to acknowledge the faculty and staff at University of Texas Pan American Mechanical Engineering Department, Dr. Miguel Paredes, Dr. Edwin LeMaster and his staff, Dr. Hashim S. Madhi and Dr. Constantine Tarawneh. A special thanks to Dr. Karen Lozano, the Plastics Lab and all the members of the Nano team.

DEDICATION

This thesis is dedicated

to the loving memory

of

Dr. Joseph Wiener PhD.

for showing me the beauty of mathematics,

to the loving memory

of

my father

Dr. Hector Mauro Lizcano M.D.

for his unwavering support and love

and

to my mother

Alma Sirenia Ramos de Lizcano

For her love and kindness.

TABLE OF CONTENTS

ABSTRACT.....	iii
ACKNOWLEDGEMENTS.....	iv
DEDICATION.....	v
TABLE OF CONTENTS.....	vi
LIST OF FIGURES.....	ix
LIST OF TABLES.....	xii
CHAPTER 1: INTRODUCTION1.....	1
REFERENCES.....	4
CHAPTER 2: ELECTORRHEOLOGICAL FLUIDS.....	5
2.1 The Electrorheological Mechanism.....	6
2.1.1 Proposed Models.....	6
2.2 Types of Effects.....	9
2.3 Formulation of ER Fluids.....	10
2.3.1 The Dispersed Phase.....	10
2.3.2 The Dispersing Phase.....	12
2.4 Concluding Remark.....	13
REFERENCES.....	14
CHAPTER 3: CHARACTERIZING ER FLUIDS.....	16
3.1 Rheology of Viscoelastic Materials.....	16

3.1.1 Geometry of Sensor and Equation Modifications.....	22
3.2 Contributing Parameters.....	23
3.2.1 Electric Field Strength and Frequency.....	23
3.2.2 Conductivity and Dielectric Properties.....	25
3.2.3 Particle Concentration.....	26
3.2.4 Temperature and Water Absorption.....	28
3.2.4 Particle Sedimentation.....	29
REFERENCES.....	30
CHAPTER 4: EXPERIMENTAL SETUP AND PROCEDURES.....	33
4.1 Materials.....	33
4.1.1 Structure and Properties C ₆₀ Fullerenes.....	33
4.1.2 Silicon Oil and Toluene.....	35
4.2 Sample Preparation.....	37
4.3 Experimental Procedure.....	40
4.3.1 Linear Viscoelastic Range and Frequency Sweep.....	40
REFERENCES.....	43
CHAPTER 5: RESULTS AND DISCUSSION.....	44
5.1 Sample 31.....	44
5.2 Sample 32.....	45
5.3 Sample 36.....	49
5.4 Sample 37.....	59
5.5 Effects of Concentration.....	67

REFERENCES.....	70
CHAPTER 6: CONCLUSIONS.....	71
APPENDIX.....	74
A: Sample 31.....	75
B: Sample 32.....	76
C: Sample 36.....	80
D: Sample 37.....	85
VITA.....	87

LIST OF FIGURES

Figure 2.1: Illustration of an ER effect [7].....	6
Figure 3.1: Spring and dashpot in parallel.....	19
Figure 3.2: Frequency sweep [8].....	21
Figure 3.3: Parallel disk sensor with top plate oscillation.....	22
Figure 4.1: A C ₆₀ fullerenes [2].....	34
Figure 4.2: C ₆₀ fullerenes crystallized into FCC cubic structure [2].....	34
Figure 4.3: Molecular structure of Toluene.....	36
Figure 4.4: Sample during processing on magnetic stirrers.....	39
Figure 4.5: Sample 37 after processing.....	39
Figure 4.6: Experimental setup.....	41
Figure 4.7: Experimental setup with mirrors and UV light.....	42
Figure 5.1: Sample 31: Storage and loss modulus vs. frequency.....	45
Figure 5.2: Storage and loss modulus vs. frequency sample 32_1.....	47
Figure 5.3: Sample 32_1 after short at 3 kV.....	47
Figure 5.4: Sample 32_1 11 minutes after short.....	48
Figure 5.5: Fibrillation and migration of particles under a dc field.....	49
Figure 5.6: Sample 36_1 ER activity.....	50
Figure 5.7: Sample 36_2 ER activity.....	50
Figure 5.8: Tan delta at different voltages for sample 36_1.....	51

Figure 5.9: Tan delta at different voltages for sample 36_2.....	51
Figure 5.10: Sample 36_1 after first short 3.2 kV.....	52
Figure 5.11: Sample 36_1 after second short at 2.8 kV.....	53
Figure 5.12: 36_1 during second short at 2.8 kV.....	53
Figure 5.13: 36_1 after third short at 2.8 kV.....	54
Figure 5.14: Difference between short sites.....	55
Figure 5.15: SEM images of (a) sample 36 and (b) 36_1.....	56
Figure 5.16: Sample 36_3 with UV light.....	57
Figure 5.17: Sample 36_5 with UV light.....	58
Figure 5.18: Fibrillation in sample 36_1.....	59
Figure 5.19: ER activity in sample 37_1.....	60
Figure 5.20: ER activity in sample 37_2.....	60
Figure 5.21: Higher voltage at 3.5 kV.....	61
Figure 5.22: Short at 3.3 kV during test.....	61
Figure 5.23: Tan delta at different voltages for sample 37_1.....	62
Figure 5.24: Tan delta at different voltages for sample 37_2.....	62
Figure 5.25: After short at 3.3 kV.....	63
Figure 5.26: G' at 0 V increases 35.7 %.....	64
Figure 5.27: G' at 0 V increases 36.7 %.....	64
Figure 5.28: G' at 0 V decreases 41.7%.....	65
Figure 5.29: G' at 0 V decreases 19.2%.....	65
Figure 5.30: Storage modulus comparison for 37_4 with application of UV light.....	66

Figure 5.31: Loss modulus comparison for 37_4 with application of UV light.....	67
Figure 5.32: G' at 0 V.....	68
Figure 5.33: G' at 1 kV.....	68
Figure 5.34: G' at 2 kV.....	69
Figure 5.35: G' at 3 kV.....	69

LIST OF TABLES

Table 4.1: Properties for molecular and crystalline C_{60} . [1], Silicon oil [5] and Toluene..	36
Table 4.2: Prepared Samples.....	38
Table 6.1: Summary of results and observations.....	73

CHAPTER 1

INTRODUCTION

Rheology is the study of the deformation and flow of matter. As a discipline, rheology, was born on April 29, 1929 in which the first meeting of the Society of Rheology was held in Columbus, Ohio [1]. Willis M. Winslow first introduced electrorheological fluids in 1949. He performed experiments with silica gel and starches in mineral oil with an applied voltage of 4 kV/mm. Results of the suspension fluid indicated that the fluid had an increase in shear resistance with an applied voltage and then returned to its original state when the electrical load was removed [2]. Applications for these types of fluids were clear to researchers, thus springing forth investigations in dampers: however, the high voltage and the abrasive effects of the silica gel cut short further research [3].

Initially, the word “electroviscous” was used to describe Winslow’s fluids, due to the increase viscosity observed in the material. It was suggested that this term was misleading in that the material did not have an increase in viscosity with an applied voltage, instead, there was an increase in the frictional forces between the plates and the fluid. Without the electric field E , the fluid between the plates responds to a load in the same manner that parallel plates separated by a thin film of oil respond. In this case,

viscosity plays a role in the movement of the plates. For the case of an applied electrical load, the fluid itself acts as a plate in contact with another plate. It is the applied electric force and the frictional forces that influence property changes in the fluid and not an increase in viscosity. The general term electrorheological or ER fluid is now used to describe Winslow's fluids [3].

ER fluids have spurred new interest because of the ability to engineer mechanical devices without mechanical parts. Possible applications range from pumps, robotic control systems and microchannels for use in MEMS devices [4, 5, 6]. Other applications include clutches, brakes and damping systems for the automotive industry [5]. Haptic actuators have already been developed for use in automobiles at Rutgers University, in collaboration with General Motors Research and Development Center [7]. Tactile arrays have also been developed for use in virtual environments that create the illusion of viscoelasticity and as aids for the visually impaired [8]. Additionally, ER fluids have applications in field-assisted polishing of micro or meso scale parts such as a micro optical lens [9]. In spite of so many applications, there are still issues with respect to required voltages needed for ER fluids to perform in a desirable manner, which is presently in the kV/mm region [4, 10].

As previously mentioned, this thesis focuses on the development and analysis of nanoparticle suspensions that exhibit electrorheological behavior under an electric field. The subsequent chapters in this work describe information obtained from literature review and experimental data. Chapter 2 covers the general topic of electrorheological

(ER) fluids including theory, behavior and composition. The parameters contributing to the behavior and the characterization of ER fluids are addressed in Chapter 3.

Experimental methods and the results are covered in Chapters 4 and 5 respectively, followed by a summation and conclusion in Chapter 6.

REFERENCES

- [1] D. Doraiswamy, DuPont iTechnologies, Experimental station, Wilmington, DE, "Origins of rheology: A short historical excursion," Nov. 2004, http://www.rheology.org/sor/publications/Rheology_B/Jan02/Origin_of_Rheology.pdf.
- [2] W. M. Winslow, "Induced fibrillation of suspensions," *Journal of Applied Physics*, vol. 20, pp. 1137-1140, Dec. 1949.
- [3] J. E. Stangroom, "Electrorheological fluids," *Physics Technology*, vol. 14, pp. 290-296, 1983.
- [4] T. Hao, "Electrorheological fluids," *Advanced Materials*, vol. 13, no. 24, pp. 1847-1857, Dec. 2001.
- [5] T. Hao, "Electrorheological suspensions," *Advances in Colloidal and Interface Science*, vol. 97, no. 1-3, pp. 1-35, March 2002.
- [6] H. A. Stone, S. Kim, "Microfluidics: Basic issues, applications, and challenges," *American Institute for Chemical Engineers Journal*, vol. 47, no. 6, pp. 1250-1254, June 2001.
- [7] J. Melli-Huber, B. Weinberg, A. Fisch, J. Nikitzuk, C. Mavroidis, C. Wampler, "Electrorheological fluidic actuators for haptic vehicular instrument controls," presented at 11th Symposium on Haptic Interface for Virtual Environment and Teleoperator Systems (HAPTICS'03), Los Angeles, CA, 2003.
- [8] P. Taylor, D. M. Pollet, A. Hoseini-Sianaki, C. J. Varley, "Advances in electrorheological fluid based tactile display," *Displays*, vol. 18, pp.135-141, Jan. 1998.
- [9] W. B. Kim, S. J. Lee, Y. J. Kim, E. S. Lee, "Electromechanical principle of electrorheological fluid-assisted polishing," *International Journal of Machine Tools and Manufacture*, vol. 43, no. 1, pp. 81-88, Jan. 2003.
- [10] K. Lozano, et al. "Electrorheological analysis of nano laden suspensions," *Journal of Colloidal and Interface Science*, vol. 297, no. 2, pp. 618-624, May 2006.

CHAPTER 2

ELECTRORHEOLOGICAL FLUIDS

Fluids are materials that flow with an applied stress and can be classified as either simple or structured fluids. Simple fluids are generally pure substances or have a uniform phase such as solutions. Structured fluids, on the other hand, have more than one phase. Their rheological behavior is governed by the interactions of its various phases. An ER fluid is considered to be a structured fluid. The interaction of a particle to other particles and to the liquid phase renders a complex rheological behavior. The addition of an electric field further increases its complexity [1, 2]. Many models have been proposed, nevertheless, they have not been able to answer many of the complexities found in these structured fluids [3]. As a result, the theory of the ER phenomenon is still under investigation.

This chapter reviews some of the models that have been proposed to explain the ER effect. Additionally, the three types of effects that have been observed are reviewed. They are the positive ER effect, the negative ER effect, and photo ER effect. Moreover, fibrillation of the particles with applied field and an electric double layer effect attributed to water has been noted. As a final point, the formulation of an ER fluid is discussed. This includes the dispersed phase and the dispersing phase. Additives are part of the

constituents of ER fluids; however, they are only mentioned in a general sense.

2.1 The Electrorheological Mechanism

The electrorheological effect takes place when a voltage is applied to a suspension fluid resulting in rheological behavioral changes. In order for a suspension fluid to have an ER effect, the fluid medium and the particulates must have certain properties [3]. In addition, the ER effect is dependant on the shear rate, applied electric field, temperature, field frequency and fluid composition, [4, 5]. The fluid formulation is discussed in section 2.3, while the other parameters mentioned are discussed in Chapter 3.

2.1.1 Proposed Models

The main characteristic of an ER fluid is the fibrillation of particles formed along the electric field, as described by Winslow [6]. Figure 1 gives a general illustration of an ER fluid before and after an electric field is applied.

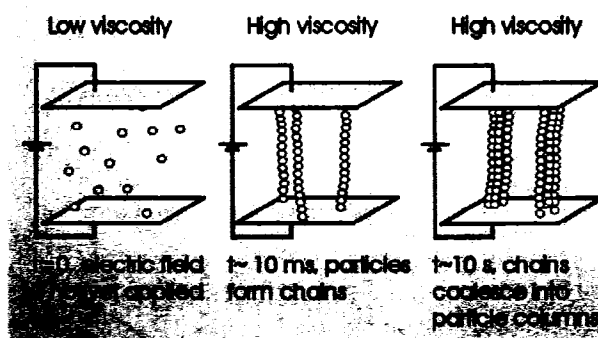


Figure 2.1: Illustration of an ER effect [7].

In a no-field state, the particles are evenly dispersed throughout the ER fluid. Within the first 10 ms of an induced E , the particles start to form chains. After 10 seconds columns are formed. In essence, the material has transformed from a fluid to a solid. The chains and columns are parallel to the electric field. When E is removed, the material recovers its initial fluid properties [8, 9]. The process is based on the induced polarization of particles due to the electric field. The ER effect is enhanced as a result of interparticle forces. The mechanism mentioned in the previous paragraph is sometimes referred as the Fibrillation Model and is a consequence of Winslow's observations, resulting in a positive ER effect [3, 6].

The electric double layer model, referred to as the EDL Model, was introduced based on the presence of water in ER suspensions. The EDL is a region in which two equal and opposite charges exist at a boundary or interface between two phases, in the case of suspensions, the liquid/particle interface. This is due to a variation of ion densities that may occur at an interface when ions, such as those from water, are present in interface systems. This model could not however, explain the overlapping of EDL with neighboring particles [3, 10].

The Water-Bridge Model was based on the migration of water ions to the surface of particles during the application of an electric field. The high surface tension of water would make the water bridge very strong. However, once anhydrous ER fluids exhibited positive ER effects, this model lost its significance [3, 11].

The polarization model is based on the parameters of the particles, the fluid, and the microstructures of the system and their relationship to the rheological properties of the whole system. Its shortcoming was that the dependence of particle conductivity and electric field frequency on the rheological properties. Moreover, the dynamic processes during change formation cannot be explained using this model [3, 12].

The conduction model was developed to overcome the limitations of the polarization model. It was based on the ratio of the particle conductivity to the liquid conductivity. It was shown to be in good agreement for many of the ER effects. The inability to explain the dynamic effects such as the ER response time has limited this model [3, 11].

In 2002, T. Hao and colleagues proposed the dielectric loss model. This model included dynamic processes in which the yield stress could be predicted based on the dielectric loss tangent that is observed in ER effect. Though his derivation has been successful for many of the parameters in an ER system, it does not account for the yield stress dependence on the electric field frequency [3].

The complexities of ER systems have made modeling extremely difficult. Nonetheless, the continual work in these dynamic materials has revealed new insight into the mechanisms of ER systems. The models presented here, though limited in some way, have provided the stepping stones for moving forward in this field of study.

2.2 Types of Effects

Three types of ER effects have been identified thus far, a positive ER effect, a negative ER effect and a photo-ER effect. When the rheological properties of an ER suspension are enhanced with an applied voltage, the system has undergone a positive ER effect. If, however, the system exhibits a decline in its rheological properties with the applied electric field, it has experienced a negative ER effect. A negative ER effect is mainly the opposite of a positive ER effect. Additionally, some systems undergo photo-ER effects (PER) when exposed to UV light [4]. Either a positive or negative photo-ER effect can occur. The most common responses reported are the positive ER effects due to its many applications [4]. A negative ER effect of nano-laden suspensions has been reported by Lozano [13].

Hao has reported characteristics of positive ER fluids. He suggests the following characteristics with an applied E , a high yield stress $\tau_y \geq 5$ kPa at 2 kV/mm, low current density, less than $2 \mu\text{A}/\text{cm}^2$, a wide temperature range between -30 and 120°C , a short response time of less than 10^{-3} s, high stability, no sedimentation, and no material degradation [4]. However, references were not identified. Wen, et al, reported an extremely high yield stress, coined GER for giant electrorheological effects. Results exhibited a yield stress of 130 kPa at 5 kV/mm for core-shell nano particles of $\text{BaTiO}(\text{C}_2\text{O}_4)_2$ coated with urea [14]. Though, the high voltage may limit its applications. Voltages currently used in ER systems are considered to be risky due to the safety and reliability concerns [13].

2.3 Formulation of ER Fluids

As mentioned ER fluids have three components; the dispersed phase, the dispersing phase, and additives. The additives are used for suspension stability and enhanced ER effect [4]. Although the additives are important, this discussion is limited to the dispersed and dispersing phases.

2.3.1 The Dispersed Phase

Another important aspect in the formulation is the particle shape, size and concentration. The dispersed phase can be either a liquid or a solid. If solid particles are used in an ER fluid, the fluid is referred to as a heterogeneous suspension fluid. A homogeneous fluid is one that uses a liquid and it referred to as a homogeneous emulsion [4]. Studies indicated that particle size, shape and concentration play a role in the type of effect an ER fluid can have. Sizes vary from 0.2 to 100 microns with various shapes including globules, flakes, granules, fragments, whiskers and general irregular shape [15-17]. The range of particles sizes mentioned have been shown to help with fluid stability. Larger particles seem to contribute to a higher yield stress, while smaller particles contribute to higher viscosities [4].

More recently, nano particles are being used as the dispersed phase. The GER system [14] discussed earlier indicated the potential of using nano particles not only for extraordinary ER effects but as nano-reinforcements as well. Nano reinforcements have

been reported to show promise as stabilizers against sedimentation and as ER enhancements [13]. Recently, the use of nanoparticles has become common place in the investigations for suitable ER fluids. Park, et al demonstrated an increase in yield stress with the use of carbon nano-particles, although not as high as those considered producing positive ER effects. A nano-composite of multi-walled carbon nano tubes (MWNT) and polyaniline (PANI) was synthesized. Stability of the MWNT was achieved with the use as polyvinyl alcohol [18]. More evidence was demonstrated using PANI clay nanoparticles with PANI particles. In this study the ER system was a hybrid mixture of micron and nano size particles [19]. It had been shown, experimentally and theoretically, that mixing particles of different materials produce a decrease in yield strength with particle of similar size. This, however, was not the case for a mixture of glass sphere particles with lead zirconate nano-particles [4]. This illustrates that the mixture of different particles in a suspension fluid may not produce a decrease in yield stress if the mixture contains both micron and nano particulates.

The geometry of the particles has been shown to have a direct bearing on the ER effect [15, 16, 20]. Hao, [4], reported that ellipsoidal shapes produce a better ER effect than spheres due to a larger electric field moment. Findings by Qi and Wen[21] showed that microsphere-based ER fluids exhibit a better ER performance, than micro-rod-based ER fluids. There is a relation between particle shape and concentration as well. The yield stress increased exponentially for ER fluids with spherical particulates and increased linearly for whisker suspensions. Thus, the performance of the ER fluid is influenced by the geometry of the particle [17].

The particle volume fractions range between 0.05 and 0.50 [4]. Results have shown that particle volume fractions between 10 and 15 % illustrate the best ER effects at temperatures within 20 ° to 25 ° C [4, 16]. Lozano, et al [13], reported a negative ER response. In her work, the particulates were carbon nano fibers at a concentration of 0.0125 wt %. Higher concentrations caused the system to short at low voltages. Increasing the temperature of an ER system has been shown to allow an increase in particle concentration. Lengalova et al [16] demonstrated that at a temperature of 60 ° C, concentration did not illustrate a maximum level for PANI base suspension with particle sizes around 20 microns. In another study, Wen, et al [14], reported a 130 kPa yield stress for nano-particle suspensions with a 30 % particle concentration at temperatures ranging from 10 ° to 120 ° C. An ER effect can be influenced by particle concentration and/or temperature, keeping in mind that the shape and size also plays a role in an ER response.

2.3.2 The Dispersing Phase

The dispersing phase is the medium in which solid or liquid particles are dispersed. They are insulating oils. In general, they consist of silicone oil, paraffin, chlorinated hydrocarbons, mineral oil, and vegetable oil. A more extensive list of common dispersing liquids can be found in literature [3, 4, 12]. The dispersing phase should exhibit high boiling points greater than 200 °C, low viscosities at less than 10 Pa·s and high densities greater than 1.2 g/cm³. Additionally, the insulating fluid should have

excellent chemical stability and preferably non-toxic [3, 4]. These fluid characteristics, with proper selection of particles, should aid in generating a positive ER effect.

2.4 Concluding Remarks

Literature has shown the importance of particle size, shape, and concentration on the type of response achieved in an ER fluid. Particle sizes have been shown to range from both micron and nano levels. Spherical shapes seem to produce a good positive ER response. Concentrations between 10 -30 % have produced favorable responses as well. It has also been noted that temperature may play a role in the maximum concentration levels that may be achieved. In addition, the dispersing phase should exhibit a high boiling temperature, low viscosities and densities greater than 1.2 g/cm^3 .

REFERENCES

- [1] A. J. Franck, "Understanding rheology of structured fluids," TA Instruments, Applications Library, New Castle, DE., Tech. Rep. AAN016 June 2005.
- [2] R. G. Larson, "Introduction to Complex Fluids," chap. 1 in *The Structure and Rheology of Complex Fluids*, NY: Oxford University Press, 1999.
- [3] T. Hao, "Electrorheological suspensions," *Advances in Colloidal and Interface Science*, vol. 97, no. 1-3, pp. 1-35, March 2002.
- [4] T. Hao, "Electrorheological fluids," *Advanced Materials*, vol. 13, no. 24, pp. 1847-1857, Dec. 2001.
- [5] H. Block, J. P. Kelly, "Electro-rheology," *Journal of Physics D: Applied Physics*, vol. 21, no.12, 1661-1677, Dec. 1988.
- [6] W. M. Winslow, "Induced fibrillation of suspensions," *Journal of Applied Physics*, vol. 20, pp. 1137-11-40, Dec. 1949.
- [7] Laboratory of Computational Engineering, Helsinki University of Technology "ER/MR phenomenon," Nov. 2004, http://www.lce.hut.fi/~alukkari/poster/ERM_R_phenomena.html.
- [8] Y. Otsubo, "Effect of electrode pattern on the column structure and yield stress of electrorheological fluids," *Journal of Colloidal and Interface Science*, vol. 190, no. 2, pp. 466-471, June 1997.
- [9] T. Hao, Z. Xu, Y. Xu, "Correlation of the dielectric properties of dispersed particles with the electrorheological effect," *Journal of Colloidal and Interface Science*, vol. 190, no.2, pp. 334-340, June 1997.
- [10] P. C. Heimenz, Raj Rajagopalan, *Principles of Colloid and Surface Chemistry*. 3rd ed., New York: Marcel Dekker Inc, 1997, pp. 499.
- [11] M. Parthasarathy, D. J. Klingenberg, "Electrorheology: Mechanisms and Models," *Material Science and Engineering: R: Reports*, vol. 17, no. 2, pp. 57-103, Oct. 1996.

- [12] K. K. Makela, "Characterization and performance of electrorheological fluids based on pine oils", PhD. Dissertation, University of Oulu, Oulu, Finland, 1999.
- [13] K. Lozano, et al. "Electrorheological analysis of nano laden suspensions," *Journal of Colloidal and Interface Science*, vol. 297, no. 2, pp. 618-624, May 2006.
- [14] W. Wen, et al, "The giant electrorheological effect in suspension of nanoparticles," *Nature Materials*, vol. 2, pp. 727-730, Nov. 2003.
- [15] A. Lengálová, V. Pavlínek, P. Sáha, O. Quadrat, J. Stejskal, "The effect of dispersed particle size and shape on the electrorheological behaviour of suspensions," *Colloids and Surfaces A: Physicochemical and Engineering Aspects*, vol. 227, 1-8, no. 1-3, pp. 1-8, Oct. 2003.
- [16] A. Lengálová, V. Pavlínek, P. Sáha, O. Quadrat, T. Kitano, J. Stejskal, "Influence of particle concentration on the electrorheological efficiency of polyaniline suspensions," *European Polymer Journal*, vol. 39, no. 4, pp. 641-645, April 2003.
- [17] Y. Otsubo, "Electrorheology of whisker suspensions," *Colloids and Surfaces A: Physicochemical and Engineering Aspects*, vol.123, no.1-3,pp. 459-466, 1999.
- [18] S.J. Park, S.Y. Park, M.S. Cho, H.J. Choi and M.S. Jhon, "Synthesis and electrorheology of multi-walled carbon nanotube/polyaniline nanoparticles," *Synthetic Metals*, vol. 152, no. 1-3, pp. 337-340, 2005.
- [19] Y. T. Lim, J. H. Park, O. O. Park, "Improved electrorheological effect in polyaniline nanocomposite suspensions," *Journal of Colloidal and Interface Science*, vol. 245, no. 1, pp. 195-203, Jan. 2002.
- [20] R. C. Kanu, M. T. Shaw, "Enhanced electrorheological fluids using anisotropic particles," *Journal of Rheology*, vol. 42, no. 3, pp. 657-670, May-June 1998.
- [21] Y. Qi, W. Wen, "Influences of geometry of particles on electrorheological fluids." *Journal of Physics. D: Applied Physics*, vol. 35, pp. 2231-2235, Aug. 2002.

CHAPTER 3

CHARACTERIZING ER FLUIDS

Rheology is an extension of solid and fluid mechanics and is used to characterize materials exhibiting plastic behavior and/or non-Newtonian behavior. Some of the nomenclature used in rheology is the shear stress, τ , the viscosity, η , the shear strain, γ , the shear strain rate, $\dot{\gamma}$, the shear storage modulus, G' , and the shear loss modulus, G'' . In the case of ER fluids, the values of the terms mentioned may be influenced by several parameters. These include the electric field strength and frequency, the conductivity and dielectric properties of the dispersed and dispersing phases, the particle concentration, temperature and sedimentation. In this chapter, the relevant rheological equations are examined, followed by contributing parameters to the ER effect [1,2].

3.1 Rheology of Viscoelastic Materials

The equations that describe the rheological characteristics of an ER fluid find their roots from Newton's law of viscometry and Hooke's law. The complex differential equations describing the deformation of fluid flow lead to a solution that is limited by boundary conditions. The boundary conditions are: the fluid must be homogeneous, and the flow must be laminar with the applied shear. If the flow is turbulent, more energy is

required and the measurements are no longer proportional to the viscosity, increasing errors up to 100%. The shear stress must be steady. A no-slip boundary condition is required so that the shear from the plate is transmitted to the liquid. If slip occurs between the plate and the liquid boundary, the shear cannot be transmitted throughout the liquid and measurements are useless [3].

When materials are subjected to an applied force, the molecules within the material rearrange as a response to the applied force. These changes within the materials can occur in a long or a short period of time. A purely elastic material is one whose response time is infinite, such as steel. The energy required to deform a purely elastic material is stored in the material and may be recovered when the applied force is removed. A purely viscous material is one whose response time is negligible compared to the time required to run an experiment, such as water. For a purely viscous material, all the energy required to deform the material is dissipated as heat [4]. Few liquids are purely viscous. They more readily exhibit a behavior that falls between a liquid and a solid. They are referred as viscoelastic materials [3]. In reality, all materials are viscoelastic, that is, they exhibit both viscous and elastic behavior [4]. ER fluids are viscoelastic materials.

Newton's law of viscosity states that the shear stress, τ , is equal to the dynamic viscosity, η , times the shear rate, $\dot{\gamma}$, or

$$\tau = \eta \times \dot{\gamma} . \quad (1)$$

The viscosity, η , is the resistance to the shear stresses and is the slope of Equation (1).

Solving for η yields

$$\eta = \frac{\tau}{\dot{\gamma}}. \quad (2)$$

The shear rate, $\dot{\gamma}$, describes the rate of deformation of the fluid and is also known as the velocity gradient. Materials whose rheological behavior obeys Newton's law of viscosity are called Newtonian fluids. Furthermore, the equation of shear rate of a material between two parallel plates is

$$\dot{\gamma} = \frac{dv}{dy} = \frac{v_{\max}}{h}, \quad (3)$$

where v_{\max} is the maximum velocity at the top of the plate/fluid interface and h is the gap between the plates [3,5].

ER fluids do not obey Newton's law of viscosity. They are referred to as non-Newtonian fluids. The linear viscoelastic property of a non-Newtonian fluid is an area where an applied deformation, γ , or deformation rate $\dot{\gamma}$, is proportionally related to the shear stress, τ , described by the Kelvin-Voight model in the following equation:

$$\tau = G\gamma + \eta\dot{\gamma}. \quad (4)$$

In this equation, G and η are the constants of proportionality, also referred to as the shear modulus and shear viscosity respectively. A mechanical analogy can be made using a spring and dashpot in parallel as in Figure 3.1, where the first term of the equation represents the spring or elastic behavior, and the second term of the equation represents the dashpot or the viscous behavior [6, 7]. Notice that for Newtonian fluids,

the first term in Equation 4 is not present.

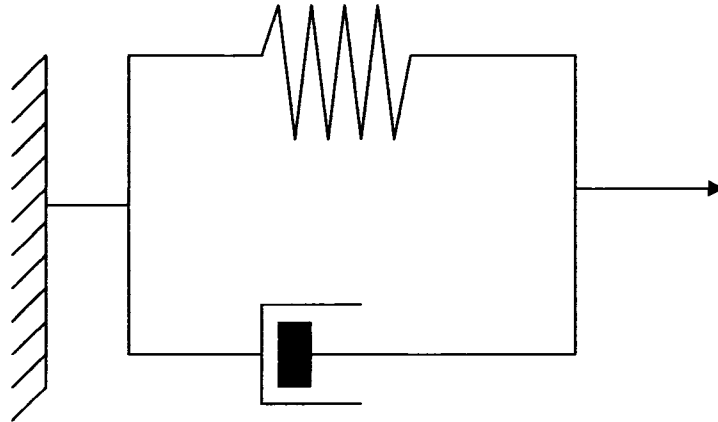


Figure 3.1: Spring and dashpot in parallel.

Rheometers are used to characterize rheological properties of viscoelastic materials. The measure of a material's linearity is referred to as the linear viscoelastic range. In general, the rheological properties are independent of the deformation, until a critical strain, γ_c is reached. As the critical strain is exceeded, the linear response becomes non-linear. In characterizing a material, a strain sweep test is first used to identify the linear viscoelastic range [8]. The deformation, γ , in this test, is sinusoidal facilitating a sinusoidal stress, τ shifted by a phase angle, δ , with respect to the strain wave. Mathematically, it is defined as follows:

$$\gamma = \gamma_o \sin \omega t , \quad (5)$$

$$\tau = \tau_o \sin(\omega t + \delta) . \quad (6)$$

Equation 6 is decomposed for analysis yielding Equation 7 and Equation 8.

$$\tau = \tau' + \tau'' = \tau_o' \sin \omega t + \tau_o'' \cos \omega t. \quad (7)$$

Trigonometric manipulation renders

$$\tan \delta = \frac{\tau_o''}{\tau_o'}. \quad (8)$$

This indicates two dynamic moduli G' , and G'' , where

$$G' = \frac{\tau_o'}{\gamma_o} \quad (9)$$

$$\text{and } G'' = \frac{\tau_o''}{\gamma_o}. \quad (10)$$

Thus, Equation 8 can be written as

$$\tan \delta = \frac{G''}{G'}. \quad (11)$$

In Equation 9, G' is the in-phase storage modulus or elastic modulus, and G'' is the out-of-phase loss modulus or viscous modulus [9]. Equation 8 and Equation 11 are referred to as the loss factor which is the ratio of the dissipated and stored energy in a sample [7]. Conceptually, during an experimental test, G' is an indication of the stress energy stored within a material used to facilitate flow that may be recovered. G'' is an indication of the unrecoverable energy used to facilitate flow, which is lost as shear heat [3].

Figure 3.2 illustrates transitions from solid to fluid behavior and fluid to solid behavior (ER effect) of a material. Strain amplitude dependence of the storage modulus, G' , and loss modulus, G'' is seen in the difference between the red and blue data lines.[8]. The red data points, with a 0.5 % strain amplitude and $G' > G''$, indicate the material behaves like a solid and the materials elastic properties are dominant. The point where the red and blue data points intersect, $G' = G''$, is a transition point where the fluid or viscous properties become dominant.

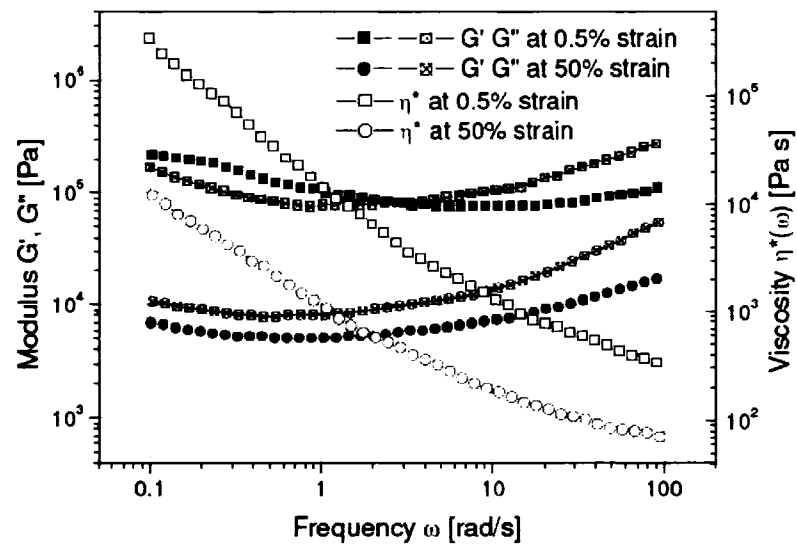


Figure 3.2: Frequency sweep [8].

At the blue data points with a 50% strain amplitude, G' and G'' do not intersect at all. In this case, the viscous properties are dominant through out the frequency sweep.

It is important to note, the linear viscoelastic range is frequency dependent. Testing at the highest and lowest frequencies of interest are therefore necessary [10].

3.1.1 Geometry of Sensor and Equation Modifications

Various sensors can be used when performing tests on a rheometer [1]. Figure 3.3 is a general representation of a parallel rotating disc sensor, which is used in the present research. The top plate oscillates at a set frequency while the bottom plate is kept stationary. The sensor measurements are determined by the disc radius, R , and the gap distance, h . The gap distance should not be smaller than 0.3mm and not greater than 3 mm. It is recommended the gap size be 3 times larger than the largest particle size [3].

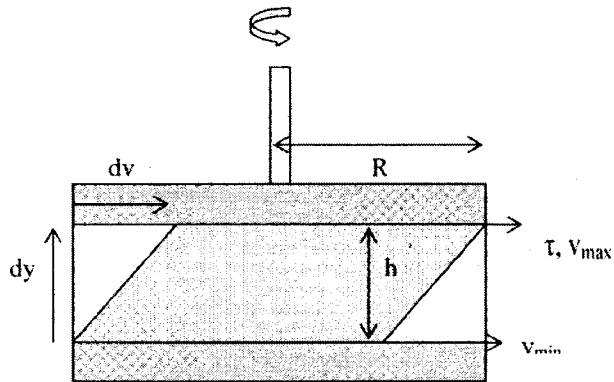


Figure 3.3: Parallel disk sensor with top plate oscillation.

For non-Newtonian fluids the shear rate must be corrected,

$$\gamma = M \times \Omega, \quad (12)$$

$$M = \frac{R}{h}, \quad (13)$$

$$\Omega = \frac{2\pi \times n}{60}. \quad (14)$$

Here, M is the geometry factor, Ω is the angular velocity, R is the radius of the disc, and n is the rotor speed in rpm. The shear stress, τ , is proportional to a geometry factor A and to the torque, T , at the outer edge of the disc, Equation (14) [3].

$$\tau = T \times A, \quad (15)$$

$$A = \frac{2}{\pi \times R^3}, \quad (16)$$

The equations discussed thus far, aids in bringing insight to the complexities of structured fluids such as and ER fluid. In subsequent chapters the experimental methods and the results and discussion will be based on these basic concepts.

3.2 Contributing Parameters

The strength of a positive ER effect can depends greatly on several parameters. These parameters deal with the electric field strength, the electric field frequency, the conductivity and dielectric properties of both phases of the system, the particle concentration, temperature and particle sedimentation. The changes in storage modulus and yield stress has been observed in relation to these parameters.

3.2.1 Electric Field Strength and Frequency

The electric field strength has a direct effect on the yield stress and is reported widely in positive ER responses [2, 11, 12, 13]. According to Hao [2], Stangroom

(1883) proposed that a critical electric field, E_C , must be overcome in order for the ER effect to take place, where the yield stress, τ_y linearly increased with increasing electric field, E , such that $\tau_y = k(E - E_C)$. In this equation k is a constant. More recently, Choi et al [11], proposed a dynamic yield stress equation where E_C is proportional to the particle conductivity. Additionally, E_C was shown to be strongly dependent on volume fraction. In this case, E_C was found to decrease with increasing volume fraction. The proposed equation is

$$\tau_y(E_o) = \alpha E^2 \left(\frac{\tanh \sqrt{E_o/E_C}}{\sqrt{\sqrt{E_o/E_C}}} \right). \quad (17)$$

It has also been reported by Tian et al [14] that the response time is proportional to the applied shear rate and with only a small dependence on the applied electric field strength. In this case, the electric field was a square wave. Furthermore, the transient process is related to the structure formation in the shearing. Tian concluded that the shear stress rose to a stable value under E when the needed shear strain was reached.

It has been shown experimentally that the electric field frequency also play a role on the ER effect. Unal et al, reported a decrease in G' with increasing frequency [15]. Cao [16], reported a decrease in τ_y when using an AC field as opposed to a DC field. Additionally, there was a significant decrease in τ_y with increasing frequency in the ac field. A decrease in τ_y from approximately 7 kPa at 20 Hz to less than 1 kPa at 1000

Hz was observed. The current density also increased when the ac field was applied and continued to increase with increasing frequency [16]. It has been proposed that particle conductivity and dielectric constant of the materials play a role in the effects of frequency on the ER response [2, 14].

The electric field strength and electric field frequency play an important role in the ER response. Typically, E_c must be surpassed in order for an ER effect to take place. An increasing particle concentration has been shown to decrease E_c . The yield stress will usually increase with increasing E . The storage modulus and the yield stress have been shown to decrease with increasing frequency. A dc field rendered a higher yield stress than an ac field. The ac field showed an increase in current density with increasing frequency. It has been suggested that these effects are due to particle conductivity and the dielectric constant of the materials. These results can aid in tailoring an ER fluids to exhibit desired properties.

3.2.2 Conductivity and Dielectric Properties

The conductivity and dielectric properties of the dispersed and dispersing phase have been shown to be related to one another and consequently affecting ER activity. The result of conductivity on an ER response can be considered in terms of the dielectric properties of the suspension fluid [2,18]. Particle conductivities between $\sigma = 10^{-12}$ to 10^{-5} S/m have been reported, with 10^{-7} S/m and 10^{-8} S/m giving the best results [2, 16,17, 18].

Zhao and Liu [17] reported a relationship between the ratios of the conductivities of particle/ liquid, σ_p / σ_L , and the ratio of the dielectric constants of particle /liquid, ϵ_p / ϵ_L . For $\sigma_p / \sigma_L > \epsilon_p / \epsilon_L$, the shear modulus is larger with DC and low frequencies. The shear modulus then drops at 10 Hz. This indicates that the polarization of the particles is dominated by the conductivity for $\sigma_p / \sigma_L > \epsilon_p / \epsilon_L$ and dominated by the dielectric properties when $\sigma_p / \sigma_L < \epsilon_p / \epsilon_L$. Similar results have been reported, as well [4, 16]. The dielectric constant of the dispersing phase must be small in comparisons to the particles. A comparatively small ER effect was found when the conductivity of the dispersing phase had a high conductivity in relation to the particle conductivity [4,19].

It can be concluded, by the evidence illustrated, that the ER response may be generated or suppressed with the manipulation of the conductivities, dielectric constants, and electric field frequencies.

3.2.3 Particle Concentration

ER response strength has been shown to increase with increasing volume fraction. In particle the yield stress increases with volume fraction and electric field strength [20, 21, 22, 23]. Hao [4, 24], has reported a critical volume fraction in which there is a sharp increment in rheological behavior when the critical volume fraction as been exceeded. Tian et al [23,] has demonstrated that the effects of volume fraction can be explained by the many body effect reported by Conrad and Wu and the conductivity

model. Furthermore, Sohm et al [20], reported the increase is due to the increase in polarization forces between particles. The increase in volume fraction does not only affect the yield stress but the storage and loss modulus is affected as well. It has been reported by Kim, that the increase volume fraction affected G' more than it affected G'' , explaining that this was due to chain formation in the suspension. The elasticity, of the suspension fluid, increased with increasing particle concentration and electric field strength [22]. In Section 3.2.1, Tian [14] reported the decrease in E_C with increasing volume fraction. However, Sung [21] reported that for a chitosan suspension in silicone oil, E_C was influenced by the conductivity mismatch between the phases of the suspension and depended very little on volume fraction. The relative viscosity increase with the application of an electric field is referred as the ER efficiency. This efficiency depends on volume fraction among other parameters. The ER efficiency has been found to increase with increasing volume fraction of the dispersed phase. Additionally, the efficiency increased with increasing temperature [24].

The volume fraction has been shown to be a critical factor in an ER response. The ER effect has been reported to show an increase with increasing particle concentration. The increase in ER strength has been attributed to the chain formation and the increase polarization forces between the particles. The critical electric field may or may not depend on the volume fraction of the particles. Furthermore, the ER efficiency has been found to increase with the increase of particles in the suspension.

3.2.4 Temperature and Water Absorption

The effect of temperature is important parameters to ER fluids because it can affect the ER response. Firstly, temperature affects the polarization intensity of particles. Particle conductivity and dielectric constant vary with temperature affecting the ability of the particles to be polarized. Furthermore, the thermal motion or the Brownian motion of the particles can increase with increasing temperature and may rupture the fibrillation formation of the suspension fluid [4, 15, 25]. A wide range of temperatures is necessary in an ER fluid in order for real world applications. Yilmaz et al [25], reported a decrease in yield stress with increasing electric field strength and temperature for PMMA-b-PSt copolymer suspensions. Xiang and Zhao [26], have reported a constant ER effect with a temperature range from 15–100° C for a MMT/TiO₂ nanocomposite.

As mentioned in Chapter 2, water may play a role in ER effect by the migration of water ions during the application of the electric field and can be effective in activating an ER response. There is however a disadvantage of water-activated ER fluids for particles that easily absorb water. As temperatures increase, the water may begin to evaporate causing instability and which may result in increasing current density. Additionally, the water may freeze at low temperatures [24, 26-29].

The effects of temperature and water are important parameters in ER activity. Increasing temperature may increase or decrease the strength of an ER Fluid.

The effect of temperature may further be affected by particle absorption of water or for water-activated ER fluids, causing thermal instability and an increase in current density with increasing temperature.

3.2.4 Particle Sedimentation

The use of ER fluids in real life applications requires a long life cycle. Commercial devices that utilize ER fluids are often limited due to particle sedimentation instability [26,30]. Sedimentation can render an ER fluid useless. A proposed remedy for preventing sedimentation is to choose particles that have a similar density as the insulating dispersing fluid. Other methods incorporate the use of surfactants to stabilize the particles. Using small particles may remedy the problem, along with the use of high viscosity insulating oils. These oils are often expensive and toxic limiting their use [26, 31]. Increasing particle concentration may provide a useful method to eliminate sedimentation problems. In this research projects, concentrations of 20, 30 and 40 weight percent are used.

REFERENCES

- [1] R. G. Larson, "Introduction to Complex Fluids," chap. 1 in *The Structure and Rheology of Complex Fluids*, New York: Oxford University Press, 1999.
- [2] T. Hao, "Electrorheological suspensions," *Advances in Colloidal and Interface Science*, vol. 97, no. 1-3, pp. 1-35, March 2002.
- [3] Schramm, Gebhard, *A Practical Approach to Rheology and Rheometry*, Karlsruhe. Gebrueder, HAAKE GmbH, 1994.
- [4] N. W. Tschoegel, *The Phenomenological Theory of Linear Viscoelastic Behavior: An Introduction*, New York: Springer-Verlag, p. 35, 1989.
- [5] A. V. Shenoy, *Rheology of Filled Polymer Systems*, Dordrecht, Kluwer: Academic Publishers, 1999.
- [6] J. W. Goodwin and R. W. Hughes, *Rheology for Chemists: An Introduction*, The Royal Society of Chemistry, pp. 98-103, 2000.
- [7] T. Mezger, *A Little Course In Rheology*, PHYSICA, Printed in Germany, pp. 40, 95, 1991.
- [8] A. J. Franck, "Understanding rheology of structured fluids," TA Instruments, Applications Library, New Castle, DE., Tech. Rep. AAN016 June 2005.
- [9] C. W. Macosko, *RHEOLOGY: Principles, Measurements, and Applications*, New York: Wiley-VCH, pp. 121-122, 1994.
- [10] HAAKE (USA), *Instruction Manual Software Rheowin Pro*, HAAKE, Printed in Germany, 2000.
- [11] H. J. Choi, I. S. Lee, J. H. Sung, B. J. Park, M. S. Jhon, "Comment on 'Preparation and electrorheological property of rare earth modified amorphous $Ba_xSr_{1-x}TiO_3$ gel electrorheological fluid,'" *Journal of Colloid and Interface Science*, vol. 295. no. 1, pp. 291-293, March 2006.

- [12] C. H. Hong, H. J. Choi, "Comment on 'The electrorheological properties of nano-sized SiO₂ particle materials doped with rare earths,'" *Scripta Materialia*, vol. 55, no. 4, pp. 415-417, Aug. 2006.
- [13] Q. Cheng, V. Pavlinek, A. Lengalova, C. Li, T. Belza, P. Saha, "Electrorheological properties of new mesoporous material with conducting polypyrrole in mesoporous silica," *Microporous and Mesoporous Materials*, pp. 193-199, May 2006.
- [14] Y. Tian, C. Li, M. Zhang, Y. Meng, S. Wen, "Transient response of an electrorheological fluid under square-wave electric field excitation," *Journal of Colloid and Interface Science*, vol. 288, no. 1, pp. 290-297, Aug. 2005.
- [15] H. I. Unal, O. Agirbas, H. Yilmaz, "Electrorheological properties of poly(Li-2-hydroxyethyl methacrylate) suspensions," *Colloids and Surfaces A: Physicochemical and Engineering Aspects*, vol. 274, no. 1-3, pp. 77-84, Feb. 2006.
- [16] J. G. Cao, M. Shen, L.W. Zhou, "Preparation and electrorheological properties of triethanolamine-modified TiO₂," *Journal of Solid State Chemistry*, vol. 179, no. 5 pp.1565-1568, May 2006.
- [17] H. Zhao, Z. Liu, "Conductivity effects in electric-field-induced electrorheological solid," *Physics Letters A*, vol. 277, no.3, pp. 175-179, Nov. 2000.
- [18] F. Ikazaki et al, "Mechanisms of electrorheology: the effect of the dielectric property," *Journal of Physics D: Applied Physics*, vol. 31, no. 3, pp. 336-347, Feb. 1998.
- [19] L. Rejon, I. Castañeda-Aranda, O. Manero, "Rheological behavior of electrorheological fluids: effect of the dielectric properties of liquid phase," *Colloids and Surfaces A: Physicochemical and Engineering Aspects*, vol. 182, no. 1-3, pp. 93-107, June 2001.
- [20] J. Sohn, J. H. Sung, H. J. Choi, M. S. Jhon, "The effect of particle concentration of poly(p-phenylene) on electrorheological response," *Journal of Applied Polymer Science*, vol. 84, no. 13, pp. 2397-2403, April 2002.
- [21] J. H. Sung, W. H. Jang, H. J. Choi, M. S. Jhon, "Universal yield stress function for biocompatible chitosan based-electrorheological fluid: Effect of particle concentration," *Polymer*, vol. 46, no. 26, pp. 12359-12365, Dec. 2005.
- [22] S. G. Kim, J. W. Kim, W. H. Jang, H. J. Choi and M. S. Jhon,, "Electrorheological characteristics of phosphate cellulose-based Suspensions," *Polymer*, vol. 42, no. 11, pp. 5005-5012, May 2001.

- [23] Yu Tian, Y. Meng, S. Wen, "Particulate volume effect in suspensions with strong electrorheological response," *Materials Letters*, vol. 57, no. 19, pp. 2807–2811, June 2003.
- [24] A. Lengálová, V. Pavlínek, P. Sába, O. Quadrat, T. Kitano, J. Stejskal, "Influence of particle concentration on the electrorheological efficiency of polyaniline suspensions," *European Polymer Journal*, vol. 39, no. 4, pp. 641-645, April 2003.
- [25] H. Yilmaz, M. Degirmenci, H. I. Unal, "Electrorheological properties of PMMA-b-PSt copolymer suspensions," *Journal of Colloid and Interface Science*, vol. 293, no. 2, pp. 489–495, Jan. 2006.
- [26] L. Xiang, X. Zhao, "Preparation of montmorillonite/titania nanocomposite and enhanced electrorheological activity," *Journal of Colloid and Interface Science*, vol. 296, no. 1, pp. 131–140. April 2006.
- [27] K. K. Makela, "Characterization and performance of electrorheological fluids based on pine oils", PhD. Dissertation, University of Oulu, Oulu, Finland, 1999.
- [28] T. Hao, "Electrorheological fluids," *Advanced Materials*, vol. 13, no. 24, pp. 1847-1857, Dec. 2001.
- [29] J. B. Yin, X. P. Zhao, "Electrorheological fluids based on glycerol-activated titania gel particles and silicone oil with high yield strength," *Journal of Colloid and Interface Science*, vol. 257, no. 2, pp. 228-236, Jan. 2003.
- [30] M. Qi, M. T. Shaw, "Sedimentation-resistant electrorheological fluids based on PVAL-coated microballoons," *Journal of Applied Polymer Science*, vol. 65, no. 3, pp. 539-547, Dec. 1998.
- [31] B. H. Sung, U. S. Choi, H. G. Jang, Y. S. Park, "Novel approach to enhance the dispersion stability of ER fluids based on hollow polyaniline sphere particle," *Colloids and Surfaces A: Physicochemical and Engineering Aspects*, vol. 274, no. 1-3, pp. 37-42, Feb. 2006.

CHAPTER 4

EXPERIMENTAL SETUP AND PROCEDURES

This chapter reviews the details of the experiment. The properties of the materials are discussed first. This is followed by a review of the sample preparation. The chapter is then concluded with an explanation of is the instrumentation and experimental methods used in this research project.

4.1 Materials

Three materials were used to make the samples. C_{60} fullerenes are the dispersed phase. The C_{60} fullerenes were purchased from BuckyUSA in and have purity greater than 99.99%. Silicon oil is the dispersing phase. Toluene is used to process the sample. Both the silicon oil and the toluene were purchased from Fisher Scientific.

4.1.1 Structure and Properties C_{60} Fullerenes

C_{60} fullerenes nanoparticles are also known as bucky balls. They were discovered by Dr. Smalley, Dr Curl and Dr, Kroto in 1985. As a result, in 1996, they shared the Nobel Prize in Chemistry.

The structure of a C_{60} fullerene is a highly symmetrical icosahedral nanostructure with a diameter of 0.71 nm. The icosahedral structure has 20 hexagonal faces with 3 double bonds and 3 single bonds and 12 pentagons with 5 single bonds. When C_{60} is in the crystalline phase it forms a FCC cubic structure and has a lattice constant of 1.417 nm [1]. Figure 4.1 and 4.2 illustrate the icosahedral and the FCC cubic structure of C_{60} .

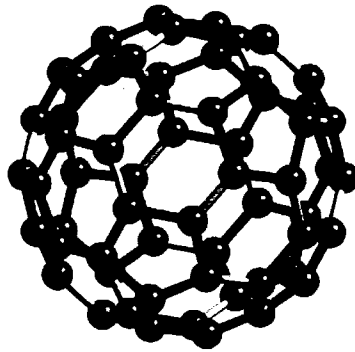


Figure 4.1: A C_{60} fullerene [2].

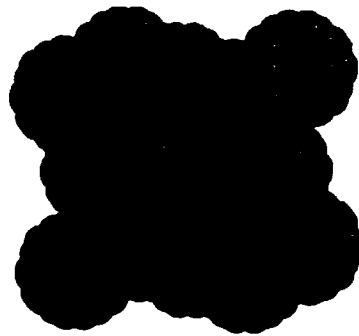


Figure 4.2: C_{60} fullerenes crystallized into FCC cubic structure [2].

The distance between two C_{60} fullerenes or nearest neighbor distance is 1.002 nm. C_{60} fullerenes have a mass density of 1.72 g/cm^3 . This is equivalent to a molecular density of $1.44 \times 10^{21} \text{ molecules/cm}^3$ [1]. The mass density of 1.65 g/cm^3 is used for this

project based on the MSDS provided by BuckyUSA which gives a mass density between 1.6 and 1.7 g/cm³. As mentioned in chapter 3, both the particle conductivity and the dielectric constant is relevant parameters in ER fluids. The particle conductivity is 1.7×10^{-7} S/cm at room temperature and the dielectric constant is 4.0-4.5. [1].

4.1.2 Silicon Oil and Toluene

Silicone oil was chosen as the dispersing phase. It is commonly used in ER fluids because it is an insulating fluid with a dielectric constant of 2.0-2.3 [3-8]. It has a weak odor and is a colorless liquid with a decomposition temperature of 250° C. Additionally, silicon oil has a density of 0.963 g/ml. The relative permittivity or dielectric constant has been found to be 2.0-2.3 and a viscosity of 50 cSt [5].

C₆₀ fullerenes are soluble in many solvents [1]. Toluene was used as a solvent for the fullerenes, as part of the sample preparation. When fullerenes are dissolved in toluene a solution is made that has a purple color. This is the color of fullerenes in a solution. There is a saturation point in which clustering will change the appearance from purple to a yellow or brown colloidal suspension (Felipe Chibante, BuckyUSA, e-mail correspondence, Sept, 1, 2005). The MSDS indicates that Toluene has a density of 0.86 g/ml. The boiling point for toluene is 110.6° C. It's molecular formula is C₇H₈. Its molecular structure, having a familiar benzene ring is shown in Figure 4.3 [9]. A summary of the physical properties relevant to this project are listed in Table 4.1 below.

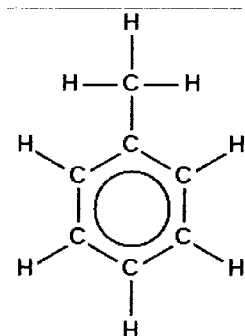


Figure 4.3: Molecular structure of Toluene.

Table 4.1: Properties for molecular and crystalline C₆₀. [1], Silicon oil [5] and Toluene.**C₆₀**

Icosahedral structure	32 faces 12 pentagons (5 single bonds) 20 hexagons (3 single & 3 double bonds)
Mean molecular diameter	d = 0.71 nm
Mass density	$\rho_m = 1.60-1.72 \text{ g/cm}^3$
Molecular density	$\rho_M = 1.44 \times 10^{21} \text{ molecules/cm}^3$
Band gap (HOMO-LUMO)	1.7 eV
Static dielectric constant	$\epsilon = 4.0-4.5$
Electrical conductivity (300 K)	$\sigma = 1.7 \times 10^{-7} \text{ S/cm}$
Thermal conductivity (300 K)	$\lambda = 0.4 \text{ W/mK}$
Melting temperature	T = 1180° C

Silicon Oil

Mass density	$\rho_m = 0.963 \text{ g/cm}^3$
Dielectric constant	$\epsilon = 2.0-2.3$
Viscosity	$\nu = 50 \text{ cSt [5]}$

Toluene

Molecular formula	C ₇ H ₈
Boiling point	110.6° C

4.2 Sample Preparation

An experimental approach was used in the sample preparation based on e-mail correspondence with Felipe Chibante (BuckyUSA) for the fullerenes and the MSDS sheet for the toluene. Toluene was used to dissolve the C₆₀ fullerenes in an effort to achieve good dispersion of the fullerenes when mixed with the silicon oil using a 1 mg/ 1 ml ratio of fullerenes to toluene.

The C₆₀ fullerenes were measured and placed in a beaker. Toluene was then added to make a solution. The solution was mixed with a magnetic stirrer for 45 minutes to 1 hour or until the particles could no longer be seen at the bottom of the beaker. The silicon oil was then added to the solution. The mixture was then homogenized for 2-3 minutes using a PRO 200 homogenizer. The magnet stirrer was then left on until the toluene had evaporated completely from the sample. Heat is added at 90° C, to aid in the evaporation process of the toluene. This temperature was chosen so that it was below the boiling temperature of the toluene. Depending on the volume of the sample, this process took between 9 to 14 days for weight fractions of 20, 30 and 40 percent. When a significant amount of toluene evaporated, the sample was placed in a smaller beaker and residue was removed from the previous beaker. The residue was removed by adding some toluene in the empty beaker until the purple color of the solution was no longer evident. This process ended when the beaker was finally changed to a 25 ml beaker. The 25 ml beaker allowed for the maximum recovery of the sample. Trying to go to a smaller beaker involved removing the sample with a rubber policeman and losing some material

or adding more toluene which defeated the purpose of placing it in a smaller beaker. The sample was then homogenized again for 2-3 minutes. Several samples were prepared and are listed in Table 4.2.

Table 4.2: Prepared Samples

Sample	weight percent of Fullerenes
31	30 %
32	20%
36	30%
37	40%

The samples were prepared as a bulk samples and labeled with consecutive numbers. Material was removed from the bulk sample and placed on the sensor of the rheometer. These samples were then labeled with the original bulk sample number, an underscore and the number of the test. For example, one bulk sample was labeled Sample 37. The first time the bulk sample was tested was labeled 37_1. Figure 4.4 is a picture of a sample after addition of the silicon oil and homogenization. Figure 4.5 is a picture of sample 37 after processing had been completed and placed on the sensor.



Figure 4.4: Sample during processing on magnetic stirrers

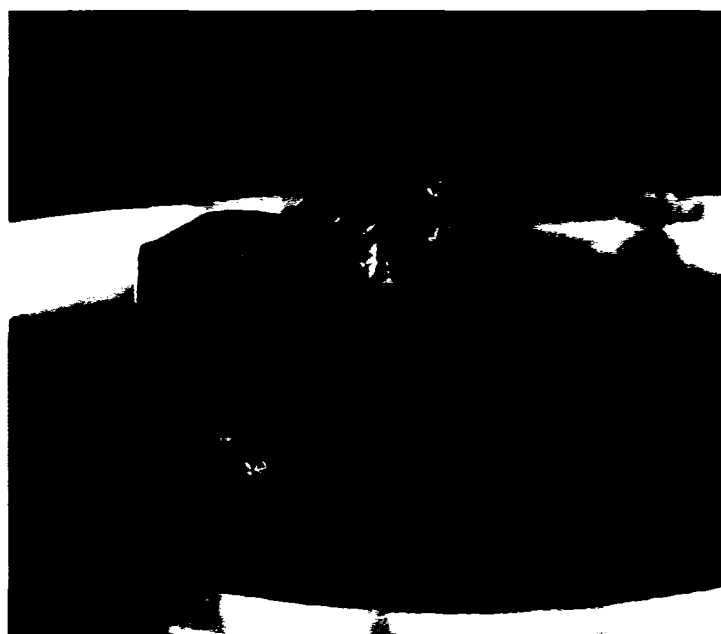


Figure 4.5: Sample 37 after processing.

4.3 Experimental Procedure

The instrumental used in this project included a rheometer, a voltage source, voltage meter, a digital camera and a digital video camera. The latter two were used later to record and capture observations noted in early experiments. All samples were tested at room temperature, approximately 24° to 26° C.

A HAAKE Rheostress RS 150 rheometer was used to perform experimental test. As mentioned in Chapter 3, a rheometer is a commonly used experimental machine in rheology when testing the rheological properties of viscoelastic materials. The following sections describe the parameters and tests used to characterize ER activity in the C₆₀/Silicon oil (C₆₀/Si) suspension samples.

4.3.1 Linear Viscoelastic Range and Frequency Sweep

The first step in characterizing the C₆₀/Si samples is measuring the critical strain, γ_c . This is the measure of the strain amplitude dependence of the storage modulus. The linear viscoelastic range of the sample is equal to or less than γ_c [10]. The test is called an Oscillating Amplitude Sweep or simply the strain sweep. The test was performed with controlled deformation for $\gamma = 0.01$ to $\gamma = 100$ at 1 Hz, 10 Hz, and 100 Hz. The gap size for all tests was 1 mm.

Next, the storage modulus and the loss modulus are measured in order to characterize the sample with and without an electric field. The test is first performed without voltage. The following test is performed with voltage. Voltage is added to the sample, while measuring the voltage input with a voltage meter. When the desired voltage is reached, the test can be started. Voltages ranged from 0 to 3.5 kV. The samples were tested over a range of oscillating frequencies with a constant oscillation amplitude that is below γ_c or in the linear viscoelastic range. In this case, the linear viscoelastic range was found to be $\gamma \leq 0.01$. The oscillating frequency sweep ranged from 1 Hz to 100 Hz. The oscillating frequency tests were performed more than once to analyze reproducibility. Furthermore, scanning electron microscopy (SEM) was performed in order to investigate structural changes in the fullerenes. The pictures, in Figure 4.6, show the experimental setup.

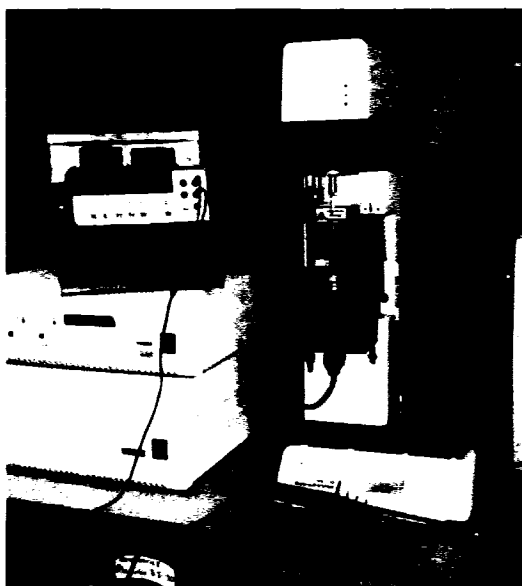


Figure 4.6: Experimental setup.

In addition to the testing mentioned above, samples 36 and 37 were tested with the addition of UV light in order to evaluate the possibility of a photo-ER effect. UV light can enhance an ER response for either a positive or negative ER effects [11]. Small square mirrors were placed around the sensor and UV light was held steady in a position such that it was reflecting off the mirrors and on the sample. Figure 4.7 illustrates the experimental setup for these tests. Additionally a video camera was used to record any visible phenomenon.



Figure 4.7: Experimental setup with mirrors and UV light.

REFERENCES

- [1] M. S. Dresselhaus and G. Desselhaus, "Fundamental properties of fullerenes," chap. 1 in *Fullerene Polymers and Fullerene Polymer Composites*, P. C. Eklund, A. M. Rao, Eds., Berlin: Springer-Verlag, 2000.
- [2] Dresselhaus Group, Massachusetts Institute of Technology, "Fullerenes," Jan. 12, 2006, <http://www.godunov.com/Bucky/fullerene.html>.
- [3] M. Parthasarathy, D. J. Klingenberg, "Electrorheology: Mechanisms and Models," *Material Science and Engineering: R: Reports*, vol. 17, no. 2, pp. 57-103, Oct. 1996.
- [4] T. Hao, "Electrorheological suspensions," *Advances in Colloidal and Interface Science*, vol. 97, no. 1-3, pp. 1-35, March 2002.
- [5] K. Lozano, et al. "Electrorheological analysis of nano laden suspensions," *Journal of Colloidal and Interface Science*, vol. 297, no. 2, pp. 618-624, May 2006.
- [6] J.G. Cao, J. Wang, L.W. Zhou, "Dielectric behavior of spinning ER particles under electric fields," *Chemical Physics Letters*, vol. 419, no. 1-3, pp. 149-153, Feb. 2006.
- [7] B. H. Sung, U. S. Choi, H. G. Jang, Y. S. Park, "Novel approach to enhance the dispersion stability of ER fluids based on hollow polyaniline sphere particle," *Colloids and Surfaces A: Physicochemical and Engineering Aspects*, vol. 274, no. 1-3, pp. 37-42, Feb. 2006.
- [8] L. Xiang, X. Zhao, "Preparation of montmorillonite/titania nanocomposite and enhanced electrorheological activity," *Journal of Colloid and Interface Science*, vol. 296, no. 1, pp. 131-140, April 2006.
- [9] The KryssTal Website, "an introduction to organic chemistry," July 2, 2006, <http://www.kryssstal.com/organic.html>.
- [10] A. J. Franck, "Understanding rheology of structured fluids," TA Instruments, Applications Library, New Castle, DE., Tech. Rep. AAN016 June 2005.
- [11] T. Hao, "Electrorheological fluids," *Advanced Materials*, vol. 13, no. 24, pp. 1847-1857, Dec. 2001.

CHAPTER 5

RESULTS AND DISCUSSION

In this chapter, the results of experimental testing are discussed alongside any observations made throughout the testing procedures. A DC field was used for all tests. Fibrillation and particle migration was observed when voltage was added to the samples. The results exhibited ER activity for all samples. One samples demonstrated a positive photo-ER effects. In some cases, a short would occur at voltages between 2.5 kV to 3.5 kV. The short would occur at either the sample site or at the power source. The short location exhibited a direct relationship to the results. SEM results revealed fiber growth for one of the samples.

5.1 Sample 31

Sample 31 had a particle weight concentration 30 %. Because the sample size was small; sample 31 was tested one time for each voltage of 0 V, 1 kV and 2kV. The effects of voltage on the storage and loss modulus as a function of frequency can be seen in Figure 5.1. The increase in G' is indicative of positive ER effect. In this case, the measurement at 1 kV gave higher values than the measurements at 2 kV. These results illustrate a favorable ER effect.

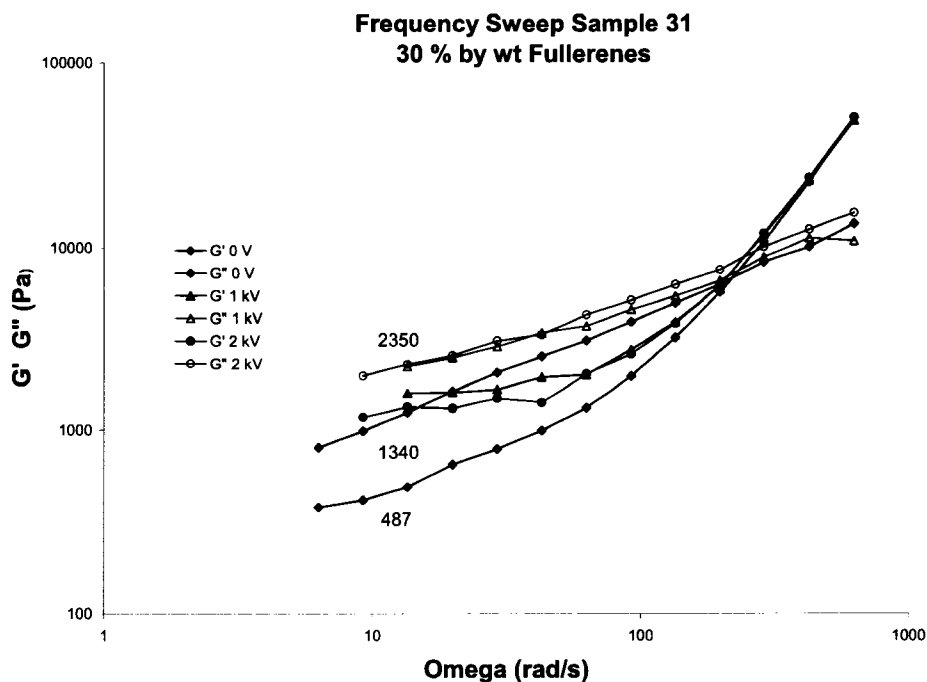


Figure 5.1: Sample 31: Storage and loss modulus vs. frequency

These effects may be attributed to the formation of columns structures and/or particle alignment. G'' also exhibited an increase, however the ratio of the loss modulus to the storage modulus is smaller with an increase of the applied field. This indicates that the elastic behavior of the material is increasing while the viscous behavior is decreasing.

5.2 Sample 32

Sample 32 had a particle weight concentration of 20 %. The lower concentration of fullerenes caused sedimentation of particles. Therefore, the sample was homogenized for 3 minutes before testing. The sample was tested at voltages of 0 V, 1 kV, 2 kV and 3 kV. The ER activity was minimal and shows a decrease in G' at 1 kV and 2kV, as

shown in the graph in Figure 5.2.

When the sample was to be tested at 3 kV, the sample shorted, displaying a flash of light. The test was then performed without voltage. The results showed a significant increase in G' without voltage than in the first test performed with voltage, as shown in Figure 5.3. At 6.28 rad/s, G' increased by 324.6 % where as G'' increased by 35.4 % and begins to decrease at approximately 3 Hz. At 100 Hz, G'' decreases by 13.2 %. This indicates that the elastic behavior was approaching the fluid behavior. In other word, the material was behaving more like a solid. This is not an indication of ER activity however. In ER fluids, the increase in storage modulus will not be present without an electric field.

The sample was tested several times at 0 V for over 11 minutes as seen in Figure 5.4. The storage modulus fluctuated from 777 Pa to 648 Pa and then up to 698 Pa. An ER effect should be reversible. In this case, the irreversibility of the sample is an induction that an ER effect has not taken place but rather something else is happening. The material may have formed some sort of structure. Voltage was then added again. While using a probe to measure the voltage input, the structure was disrupted and values of the storage and loss moduli were similar to the initial values at 0 V, 1 kV and 2kV. Thus, irreversibility only lasted as long as the sensor remained undisturbed.

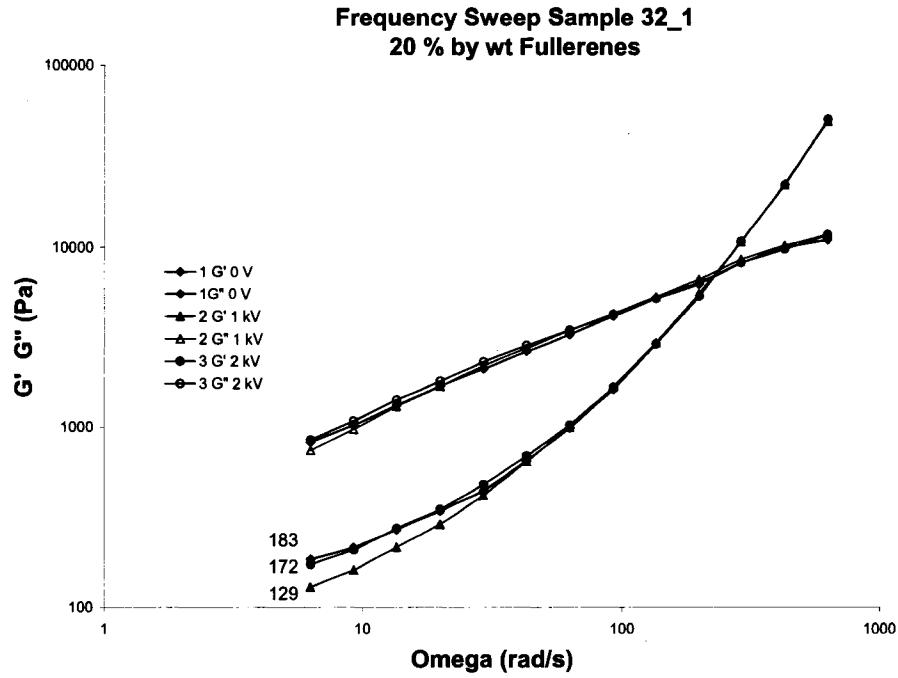


Figure 5.2: Storage and loss modulus vs. frequency sample 32_1.

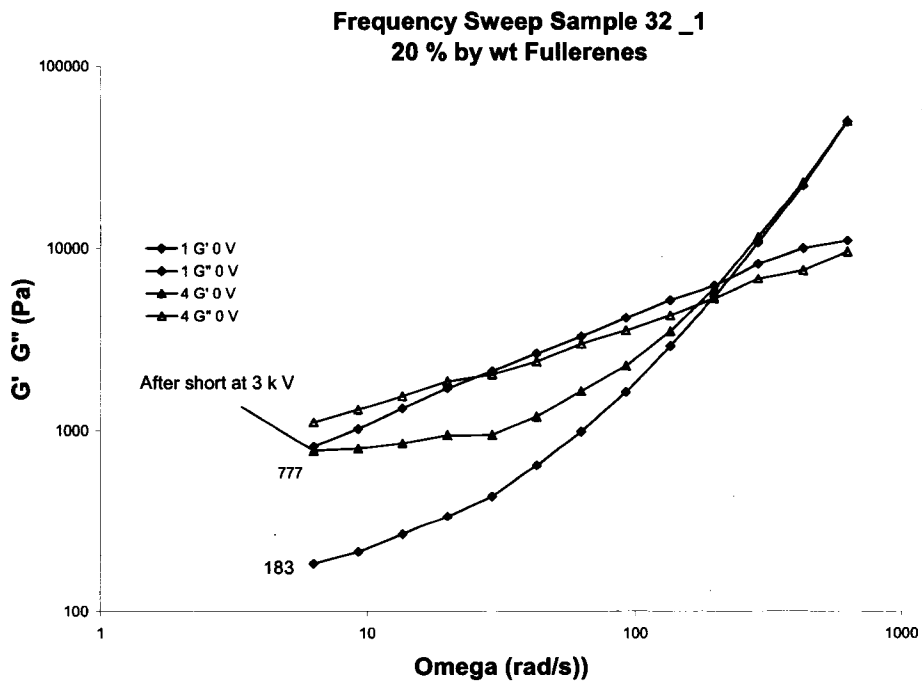


Figure 5.3: Sample 32_1 after short at 3 kV.

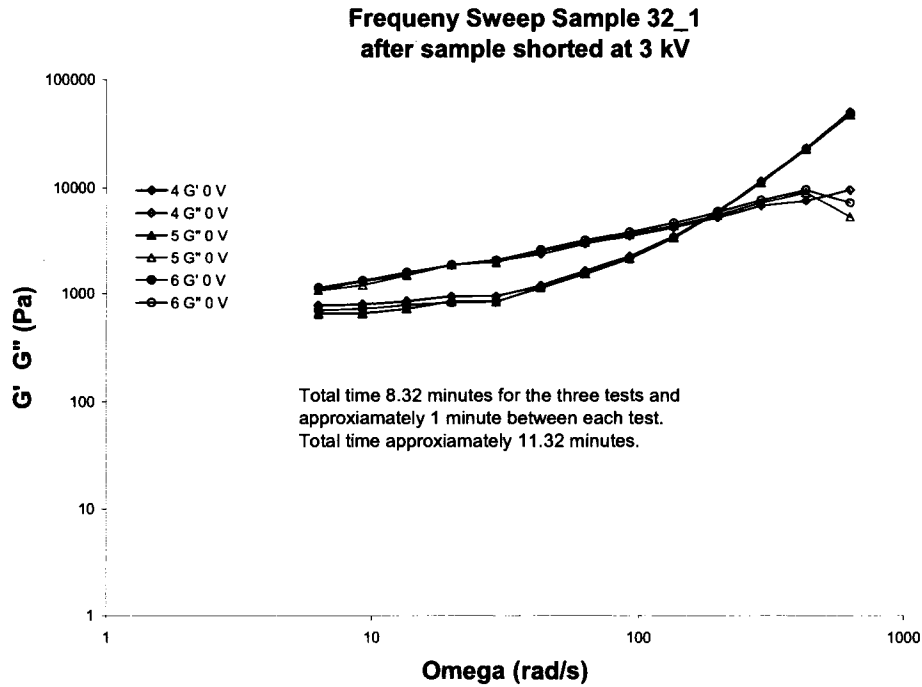


Figure 5.4: Sample 32_1 11 minutes after short.

In addition to the changes in the storage and loss modulus, fibrillation and migration of particles was observed when voltage was added slowly and held steady below 2.8 kV. The sample also appeared to oscillate within the sensor plates. In another experiment, voltage was added to the sensor without running a test to observe and record this phenomenon. Figure 5.5 illustrates the fibrillation and migration of particles to the top plate of the sensor edge. The fibrillation may be a result of the dipole-dipole interactions of the particles induced by the electric force. The particle migration and the movement of the sample may be a result of electrophoresis in which the particles have a surface charge. Similar observations were reported by Espin, et al [1].



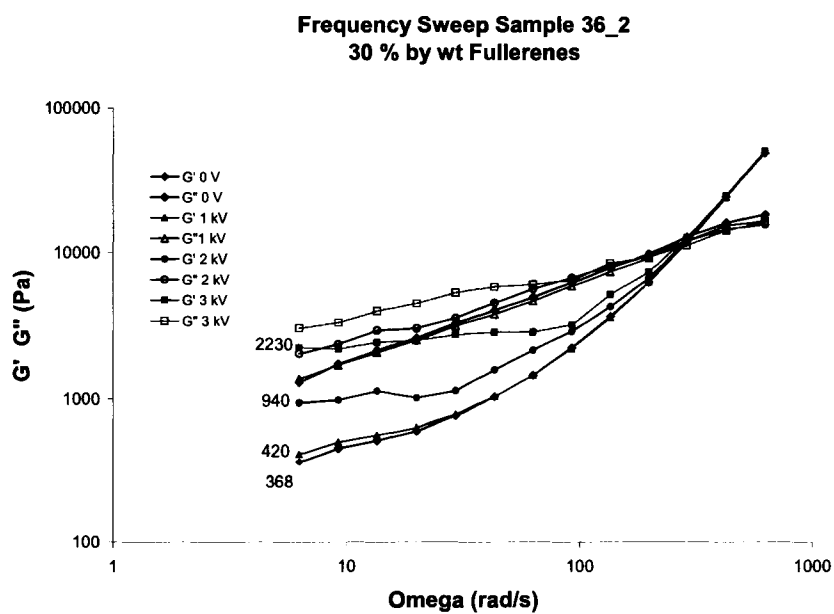
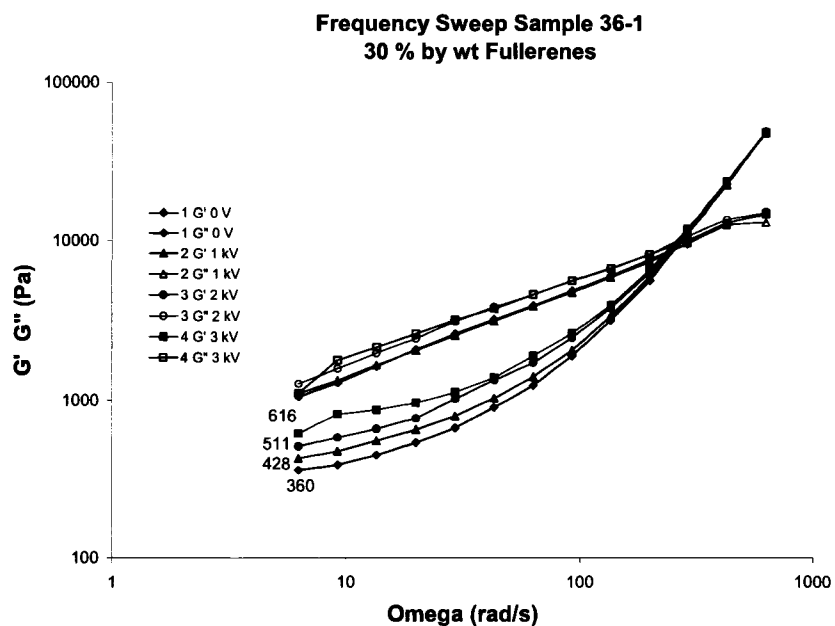
Figure 5.5: Fibrillation and migration of particles under a dc field.

5.3 Sample 36

Sample 36 had a particle concentration of 30 % and was a paste similar to sample 31. Sample exhibited ER activity and photo-ER activity with the application of UV light. The sample shorted at the sample site and at the power source. Differences in the results were observed depending on the short site. Additionally, fibrillation was visible.

Sample 36_1 and 36_2 were tested several times at voltages ranging from 0 V to 3.2 kV. Figure 5.6 and Figure 5.7 demonstrates positive ER activity in these samples. G' increased with increasing voltage. While G'' also increases with increasing voltage, it is not as significant as in the storage modulus. This is described by the loss factor, $\tan \delta$ from Equation 11 in chapter 3. If $\tan \delta > 1$ then the viscous behavior dominates the system, for $\tan \delta < 1$ indicates elastic behavior dominates the system [2]. It is reasonable to expect a better ER response due to the higher concentration of particles when compared to the sample 32. The loss tangent is shown for both 36_1 and 396_2. Figure 5.8 and

Figure 5.9 shows $\tan \delta$ as a function of frequency. They describe the decreasing viscous behavior with increasing voltage.



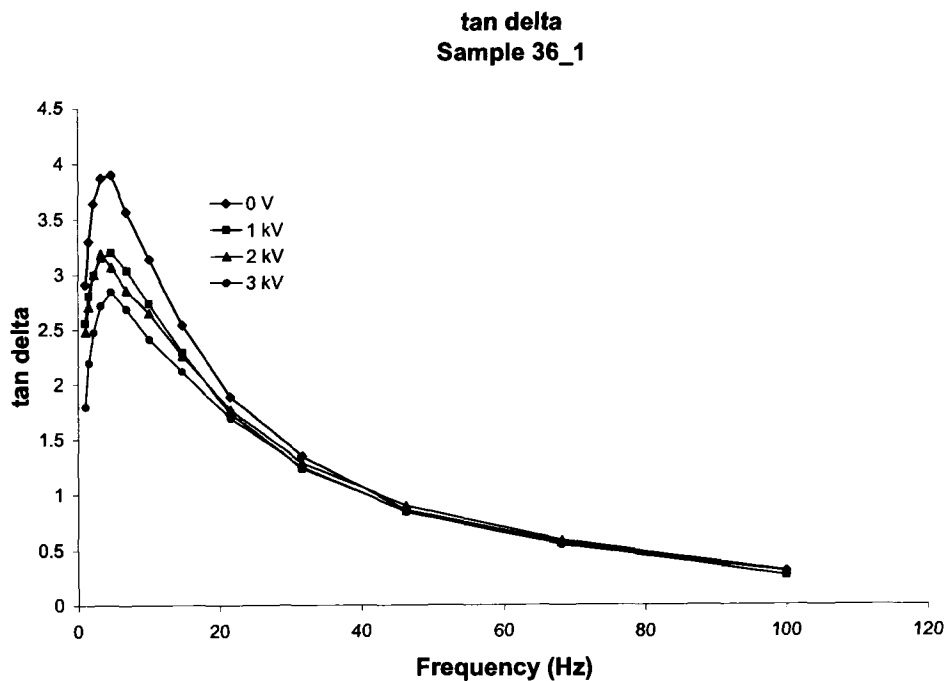


Figure 5.8: Tan delta at different voltages for sample 36_1.

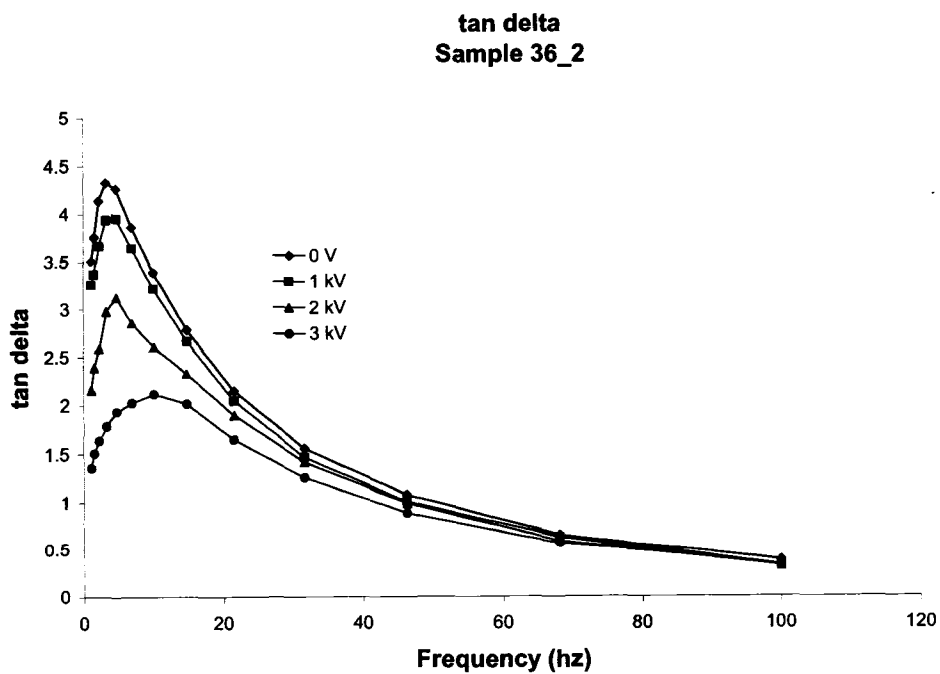


Figure 5.9: Tan delta at different voltages for sample 36_2.

A difference was noted between the shorts occurring at the sample site or shorts occurring at the power source. Furthermore, the intensity of the short at the sample site produced varying results. The first short occurred at 3.2 kV. An increase in G' can be seen in Figure 5.10. A second short occurred at 2.8 kV. In this case, the short was considerably more intense than in the first short at 3.2 kV. G' exceeded G'' indicating the elastic behavior dominated the system. This is shown in Figure 5.11. Figure 5.12 is a photo captured from video of the flash of light during the second short.

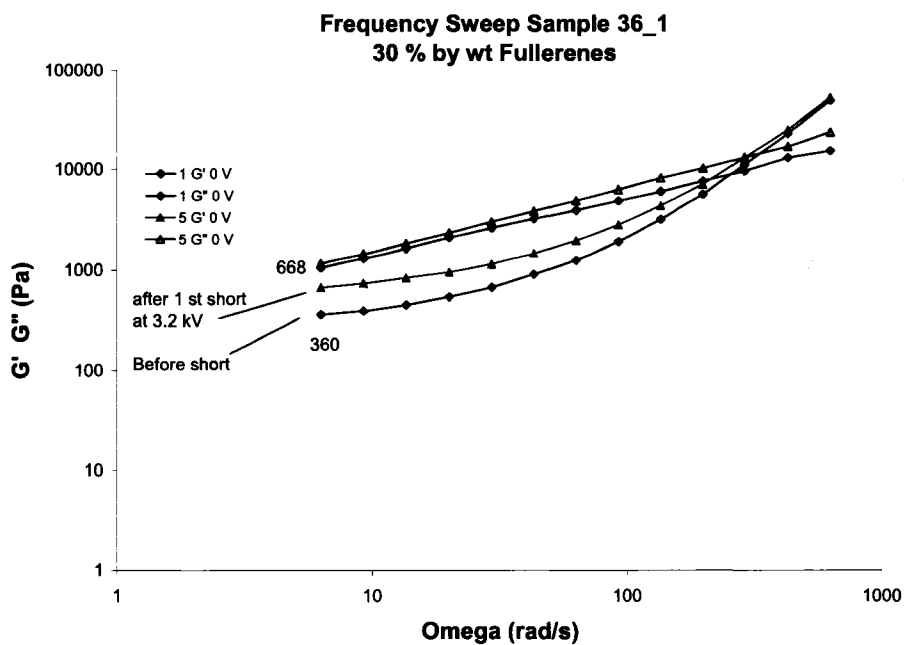


Figure 5.10: Sample 36_1 after first short 3.2 kV.

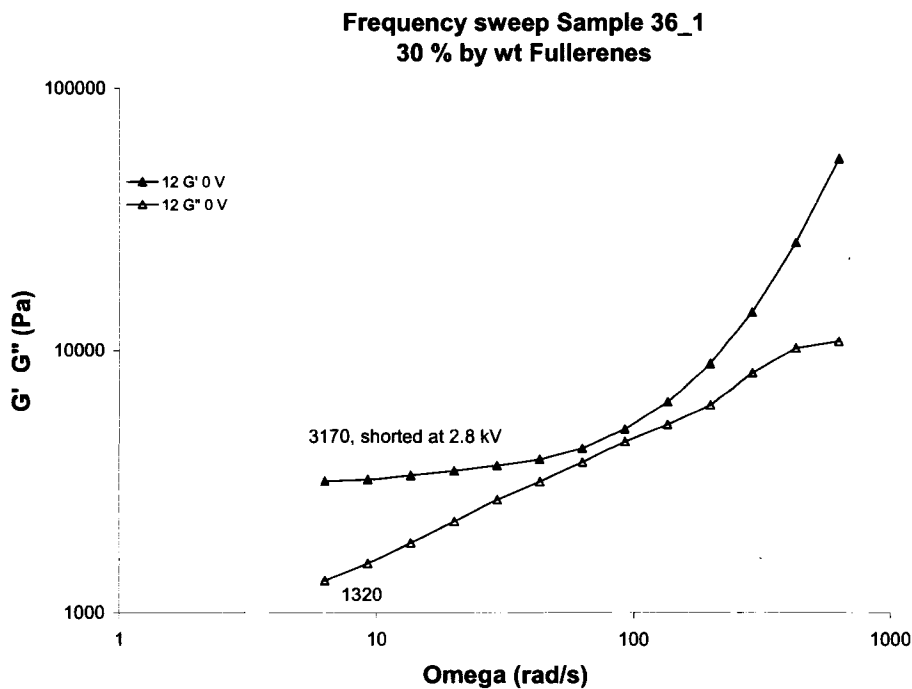


Figure 5.11: Sample 36_1 after second short at 2.8 kV.



Figure 5.12: 36_1 during second short at 2.8 kV.

Third short yielded an increase in both G' and G'' at the same voltage as the second short of 2.8 kV, however it was not as intense and the values for the storage moduli were significantly lower. The loss modulus was higher than the previous short. Figure 5.13 is a graph of the frequency sweep after the third short.

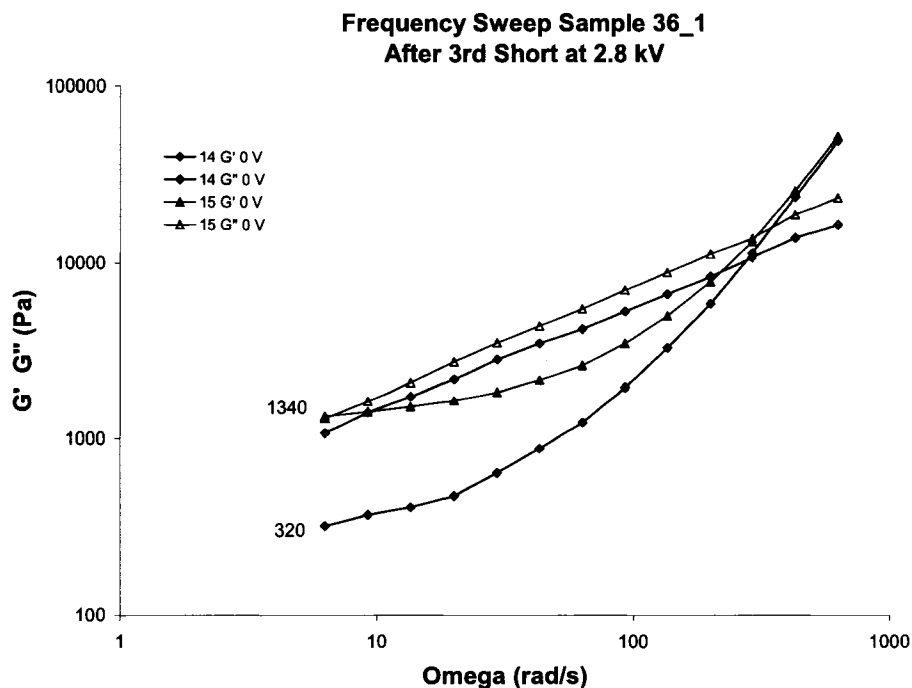


Figure 5.13: 36_1 after third short at 2.8 kV.

In another test, 36_1a shorted at the sample site and at the power source. Figure 5.14 shows the difference in the values of G' and G'' for each location of the short. In this case, the short at the sample site occurred at 2.8 kV and the short at the power source occurred at 3 kV. This was the second short for this sample. The difference is an indication that the light emitted during a short may be responsible for the behavior of the material and that the short itself is not as important. The emission of light may be an electroluminescence in which electric field induced excitation of electrons release energy in the form of photons. Single C_{60} crystals have been reported to exhibit electroluminescent behavior [3]. Another explanation may be that of an electrical arc

discharge. The light emission of an electric arc falls in the range of ultraviolet light. It is similar to light emissions in electric arc discharges in welding [4, 5].

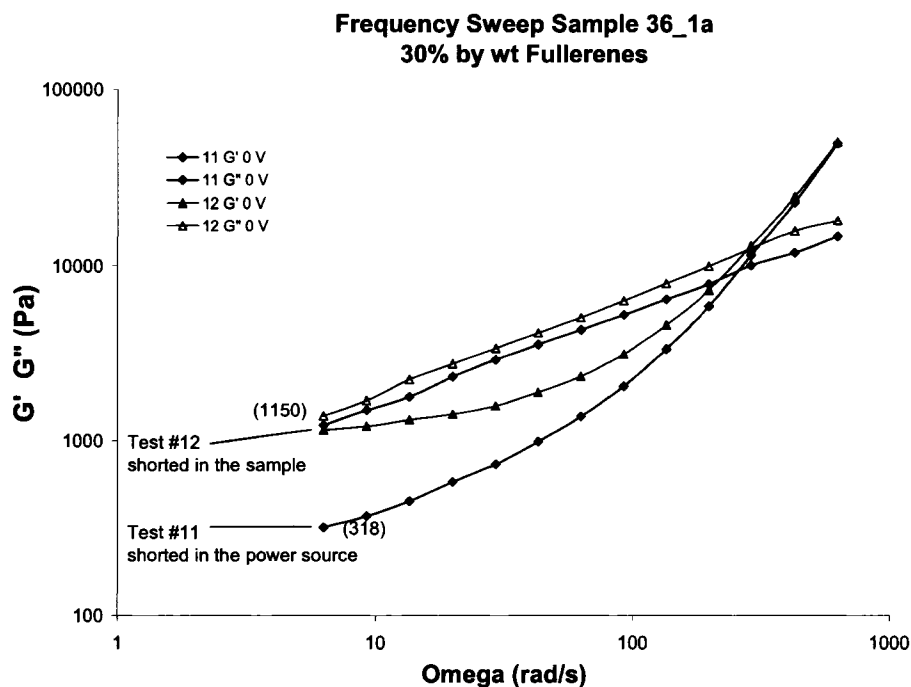
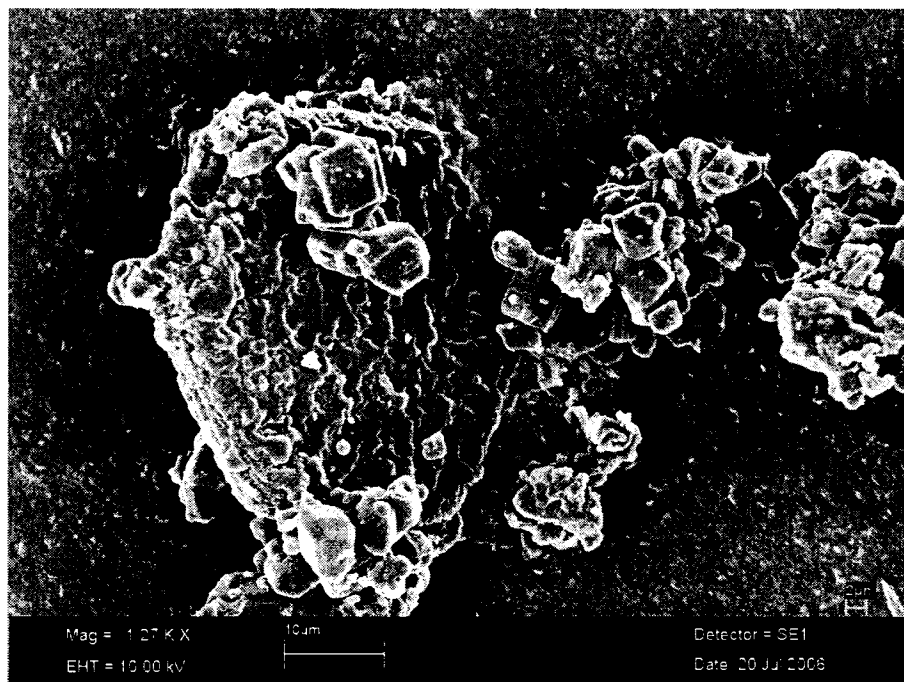
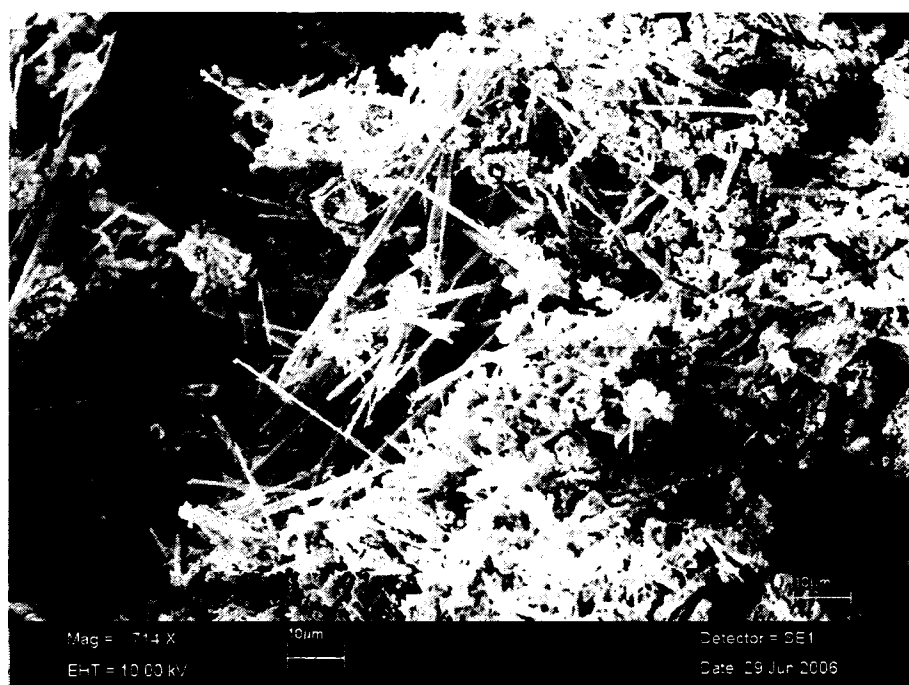


Figure 5.14: Difference between short sites.

C_{60} exposed to visible or UV light in an oxygen free environment, under high pressure and high temperature (HPHT) and in other cases, at 300 K, polymerizes the fullerenes [6, 7]. Although the samples in this case are exposed to oxygen and are not under HPHT conditions, the silicon oil may provide a suitable environment for polymerization of the fullerenes. SEM pictures of 36_1 supports the possibility of polymerization as shown in Figure 5.15. The first image is of sample 36 before any testing is performed. The second image is of 36_1 after testing. A large amount of fibers can be seen that are a result of the phenomenon observed during testing.



(a)



(b)

Figure 5.15: SEM images of (a) sample 36 and (b) 36_1.

The effects of UV light were further investigated. The results indicate a positive photo-ER activity as shown in Figure 5.16. The values of G' and G'' are similar to those for samples 36_1 and 36_2 at 1 kV. G' increases by 57.4 % at 2 kV and increases by 35.9 % at 3 kV. These results were not reproducible past 2 kV in 36_5. The sample kept shorting between 2.5 kV and 2.8 kV. Furthermore, the UV light was a small hand held device that was clamped down and placed in a position so that it reflected off mirrors surrounding the sensor. It is possible that the UV light might not have been reflecting light in a similar fashion as for 36_3. Figure 5.16 shows an increase in G' at 2 kV as well for sample 36_5 in Figure 5.17.

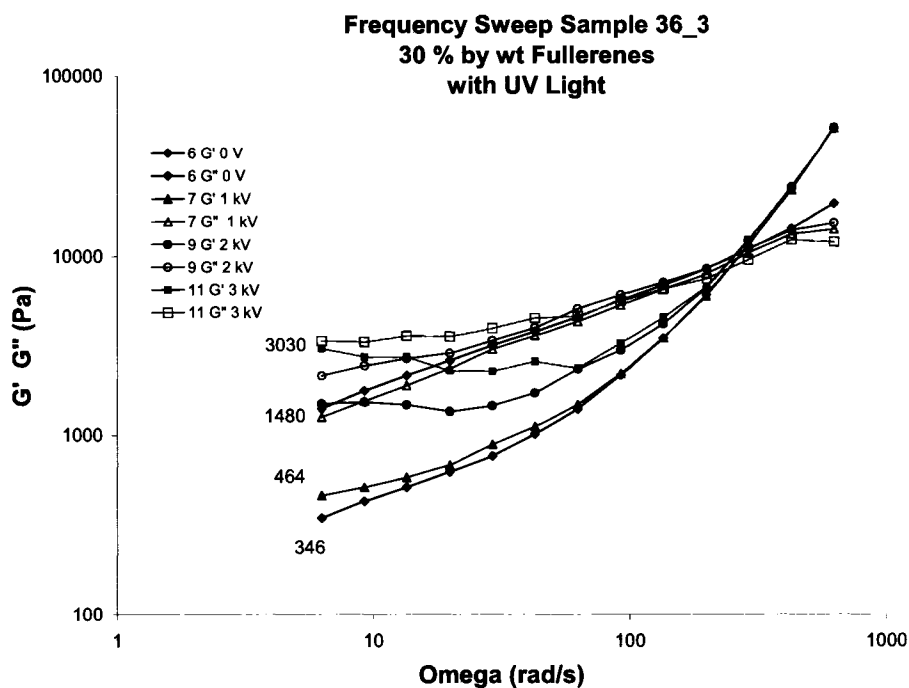


Figure 5.16: Sample 36_3 with UV light.

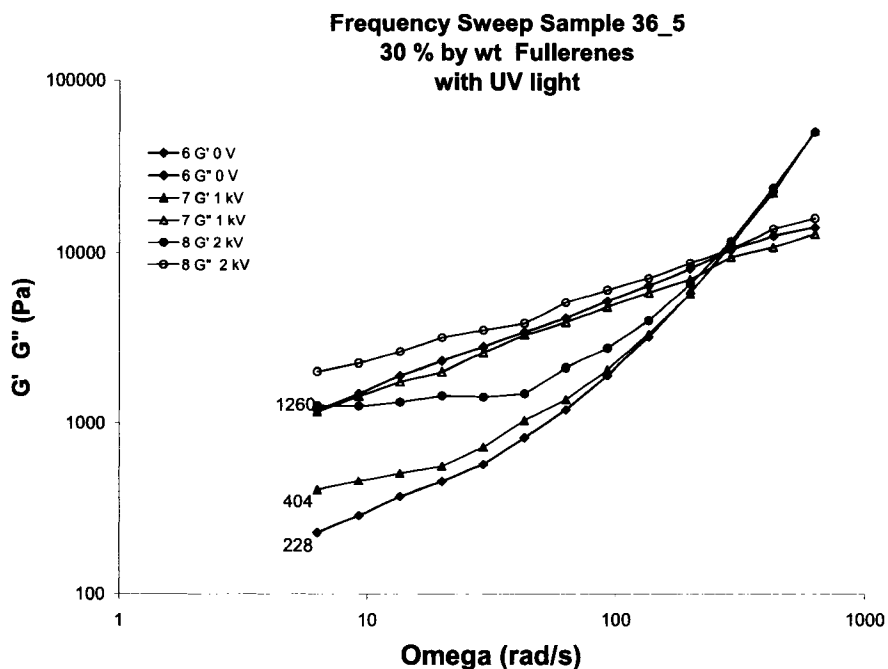


Figure 5.17: Sample 36_5 with UV light.

As in sample 32, fibrillation was visible in sample 36_1 and is shown in Figure 5.18. Some particle migration can be seen at the bottom right side of the sensor edge; however, it was less than in sample 32. Fibrillation can be seen throughout the sample but is most evident on the right side of the sensor. It is interesting to note that the fibrillation appears to be on the upper side of the sensor throughout the middle and left side of the sensor. This may be caused by distortions on the video from a clear plastic film that is placed in front of the camera to prevent any spatter from landing on the lens.

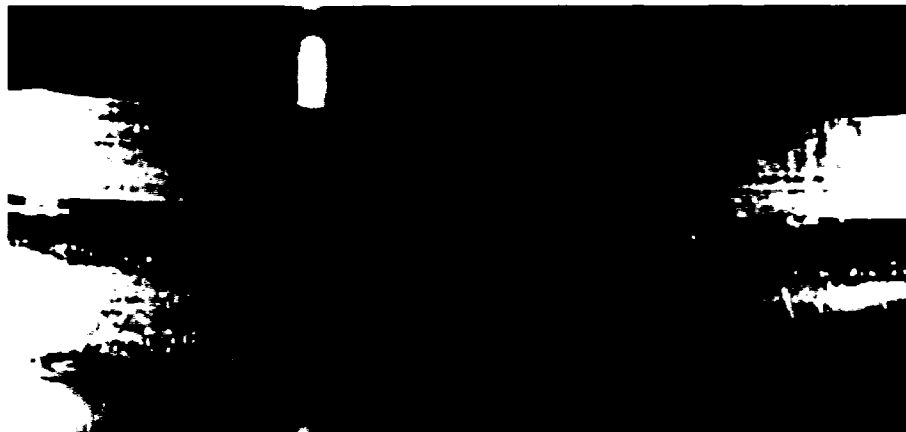
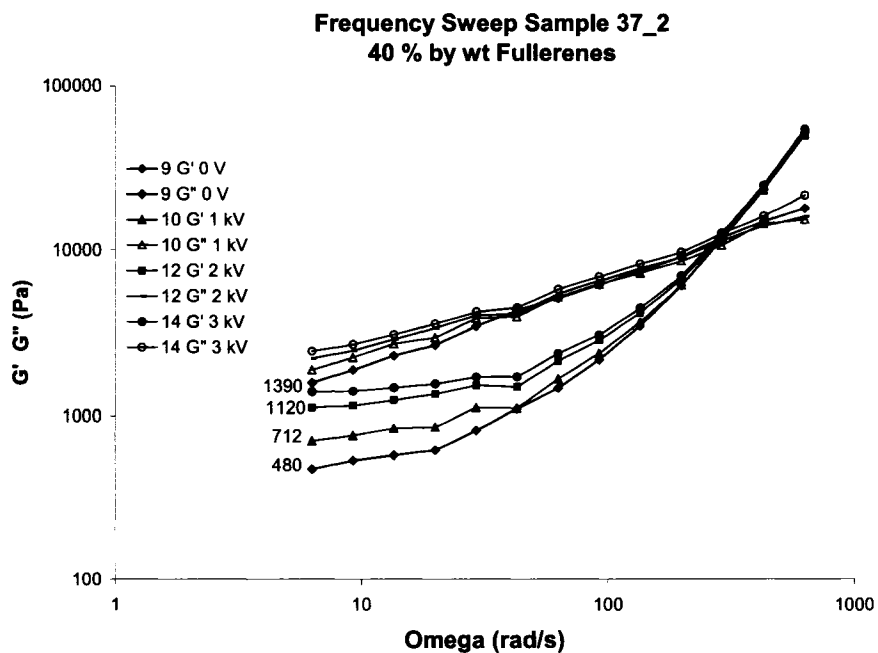
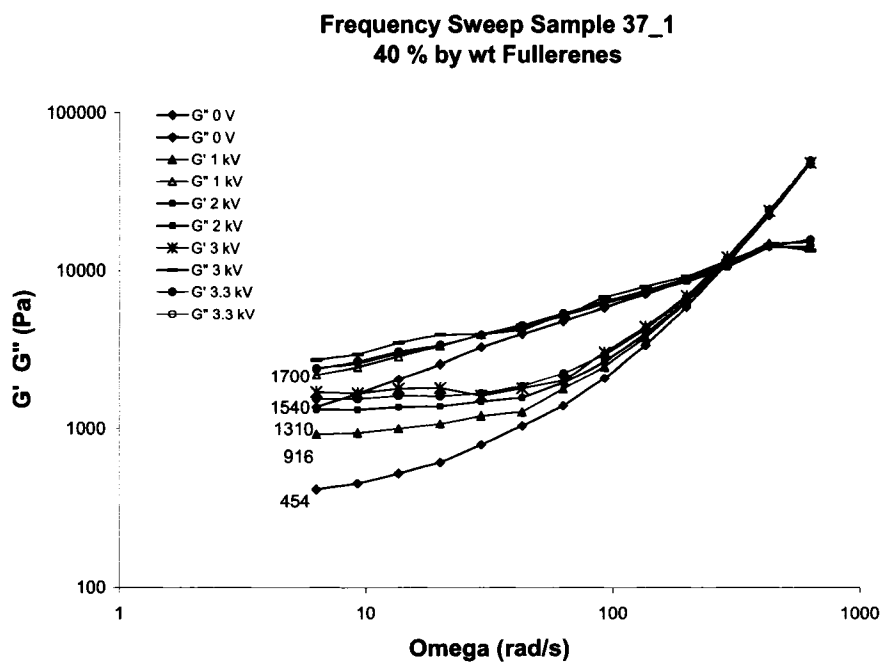


Figure 5.18: Fibrillation in sample 36_1.

5.4 Sample 37

Sample 37 had a particle weight concentration of 40 % and was a paste similar to samples 31 and 36. ER activity was observed in sample 37_1 and 37_2 as seen in Figure 5.19 and Figure 5.20 respectively. Additionally, a higher voltage was achieved up to 3.5 kV as seen in Figure 5.21 for sample 37_2. Sample 37_1 shorted once at 3.3 kV during a test at approximately 10 Hz shown in Figure 5.22. The values exhibited erratic behavior and the data did not provide useful information. Figure 5.23 and Figure 5.24 shows the loss tangent decreasing with increasing voltage for Samples 37_1 and 37_2 with the largest decreases from 0V to 1 kV and then from 1 kV to 2 kV. This indicates that the percent increase in G'' become smaller with increasing voltage.



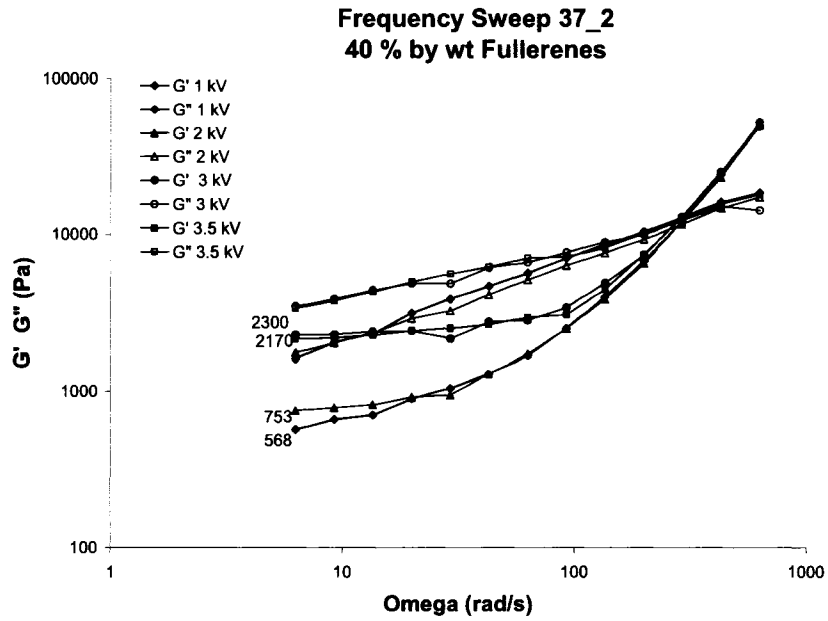


Figure 5.21: Higher voltage at 3.5 kV.

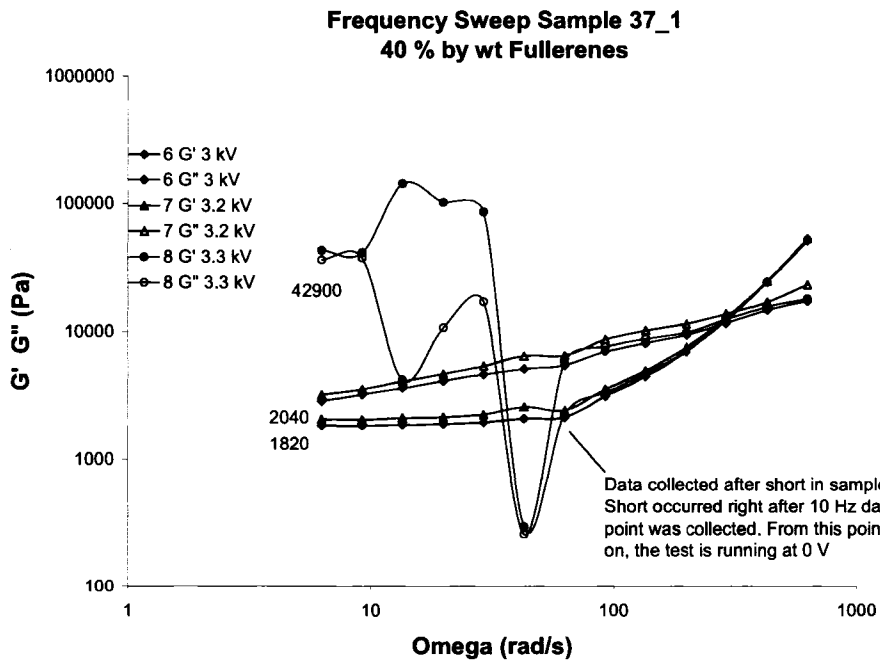


Figure 5.22: Short at 3.3 kV during test

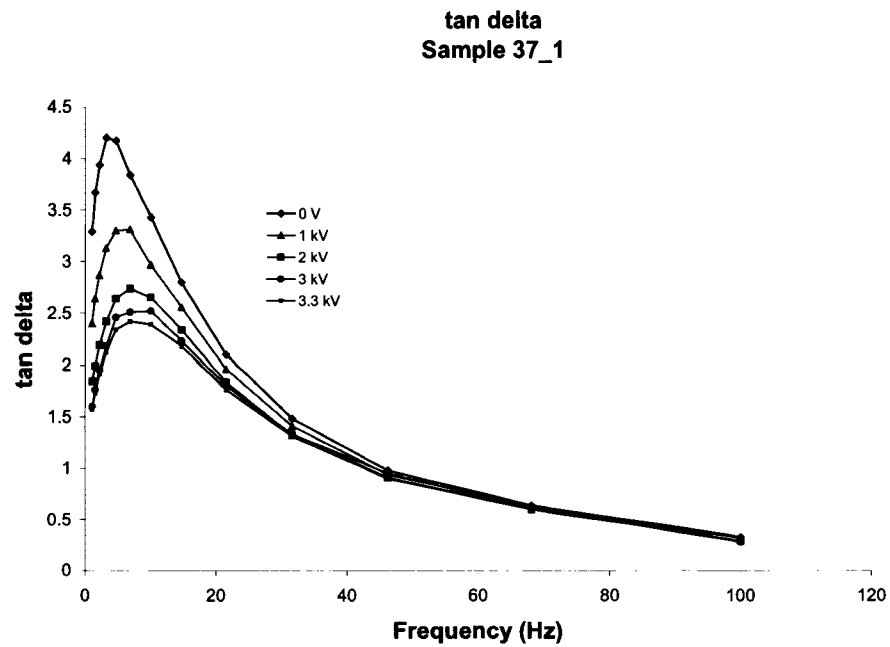


Figure 5.23: Tan delta at different voltages for sample 37_1.

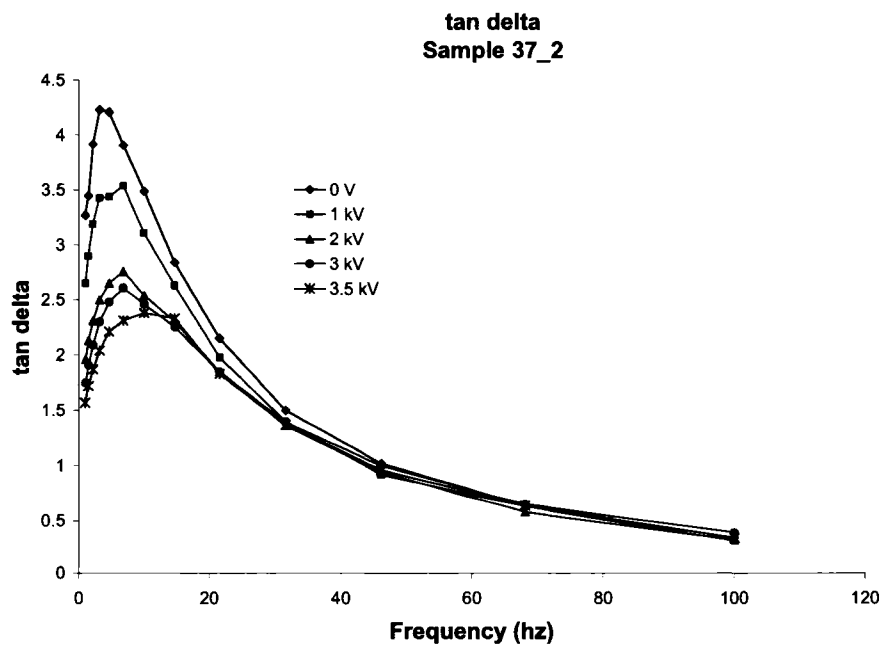


Figure 5.24: Tan delta at different voltages for sample 37_2.

After the sample shorted at 3.3 kV, tests were run at 0 V, 1 kV, 2 kV, 3 kV, 3.2 kV, 3.3 kV. The sample was tested at 0 V, before increasing the voltage. It was observed that as the voltage increased the subsequent values of G' at 0 V increased when compared to the previous value at 0 V. This occurred up to 3 kV. At 3.2 kV, G' started to decrease for values with voltage and without voltage. These results are shown in Figure 5.25, Figure 5.26, Figure 5.27, Figure 5.28 and Figure 5.29. These changes indicates that the ER activity is not reversible and the residual column structures and/or particle alignment may be occurring.

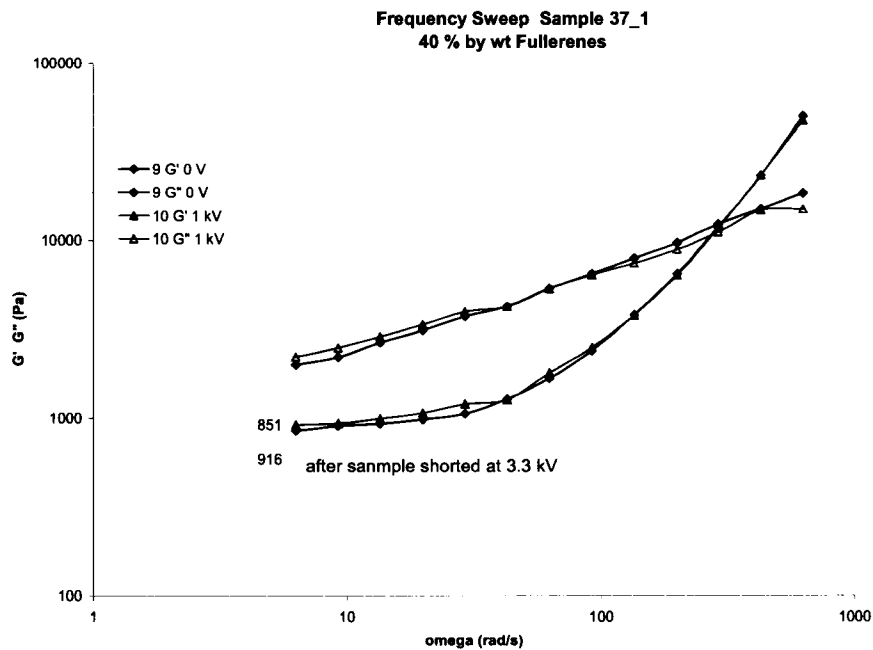
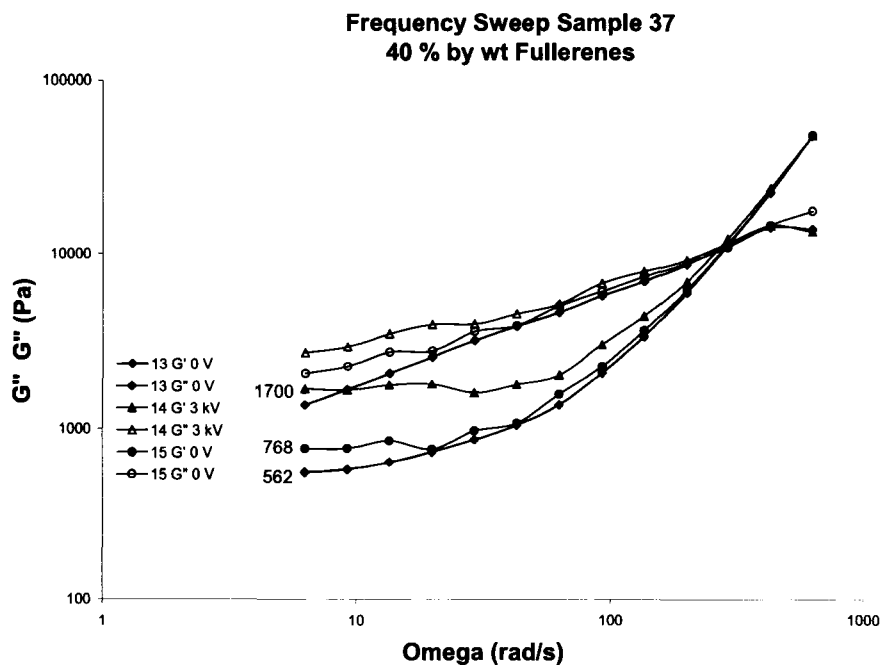
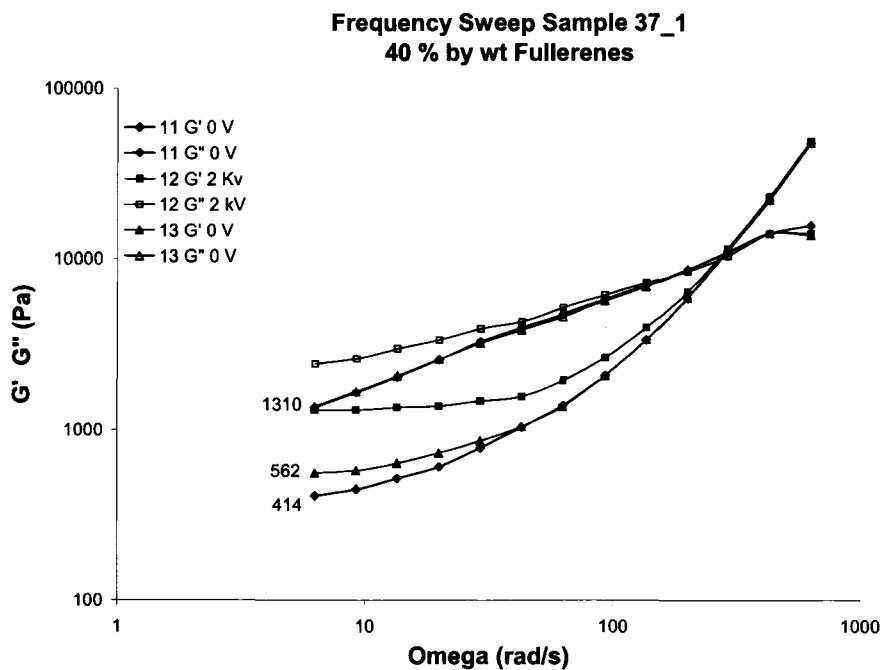


Figure 5.25: After short at 3.3 kV.



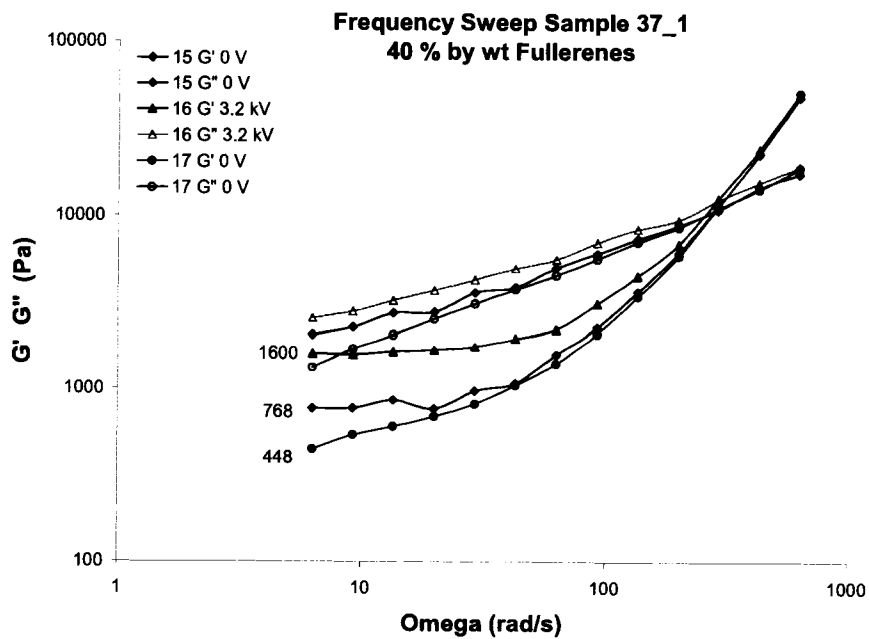


Figure 5.28: G' at 0 V decreases 41.7%.

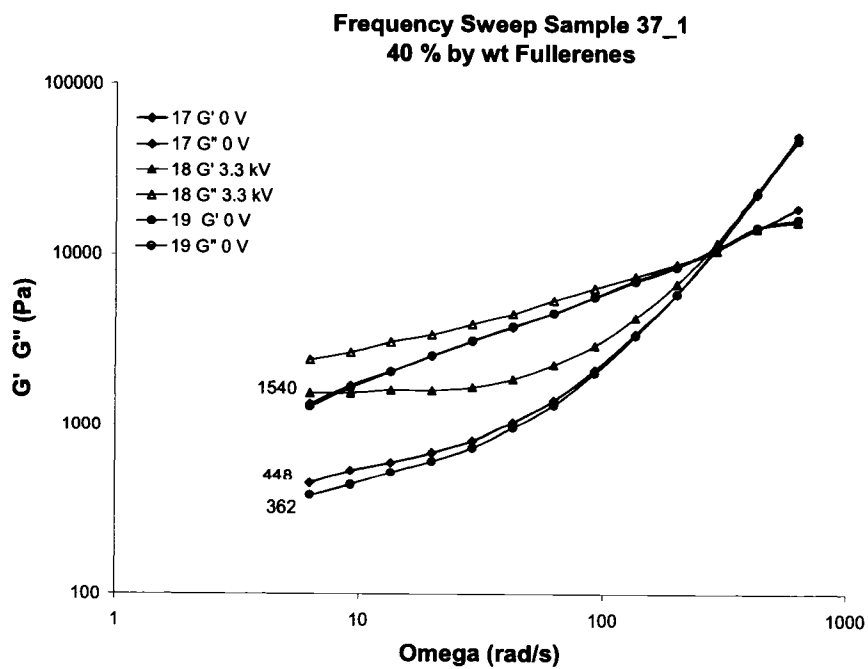


Figure 5.29: G' at 0 V decreases 19.2%.

A photo-ER activity was observed in sample 37_4 at 1 kV. However, it is not as significant as in sample 36_3. This may be due to the higher concentration of fullerenes. This might make it more difficult for the ultraviolet light to go through the material. The results are shown in Figure 5.30 and Figure 5.31. Better results may be obtained with a glass electrode that would allow the UV light to penetrate a larger surface area.

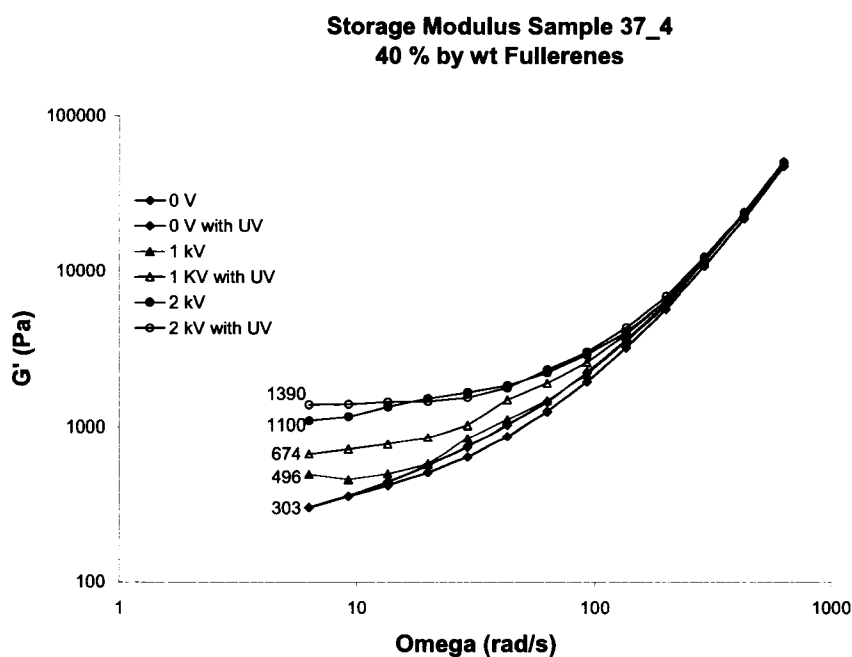


Figure 5.30: Storage modulus comparison for 37_4 with application of UV light.

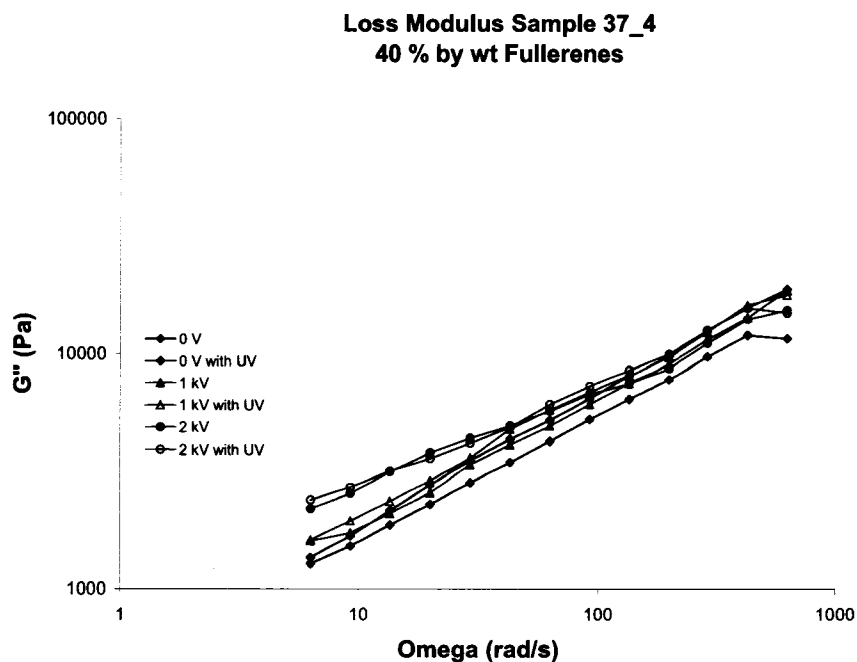


Figure 5.31: Loss modulus comparison for 37_4 with application of UV light.

5.5 EFFECTS OF CONCENTRATION

Three weight fractions were investigated. A relationship between ER effects and the particle concentrations were observed. Samples 36 and 37 had a similar response without an electric field as seen in Figure 5.32. When the voltage is increased to 1 kV and 2 kV, Sample 37 has a better response than samples 32 and 36. This can be seen in Figure 5.33. Sample 36 has a larger response than sample 32 at 1 kV and 2 kV. This is expected with increased particles available for polarization, thus, increasing the number of column structures. In Figure 5.34, a significant increase in the storage modulus is observed. Additionally, sample 36 had a significantly larger response than sample 37 at 3

kV as seen in Figure 5.35. A critical concentration may have been exceeded in sample 37 for an electric field at 3 kV. On the other hand, voltages up to 3.5 kV were achieved in sample 37, whereas sample 36 would short for voltages higher than 3 kV.

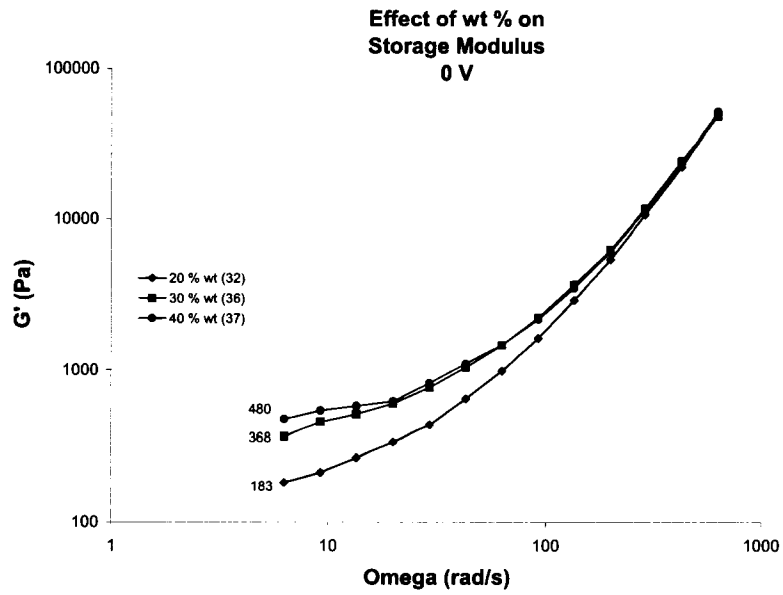


Figure 5.32: G' at 0 V.

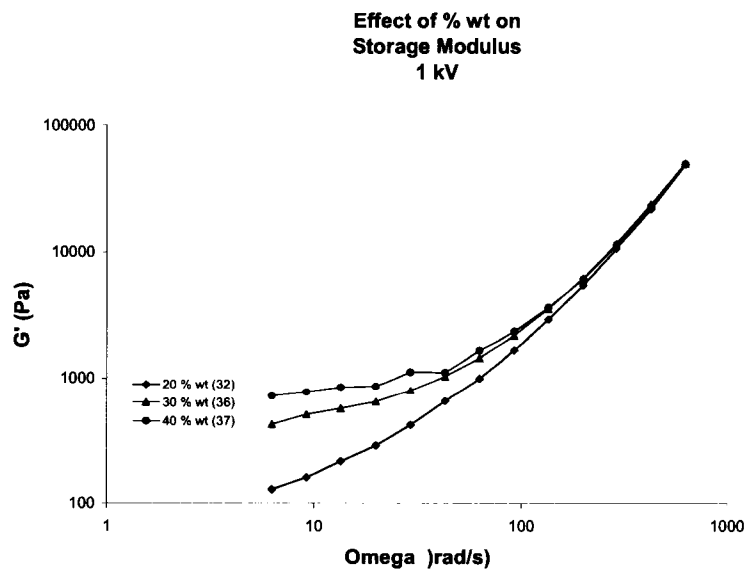
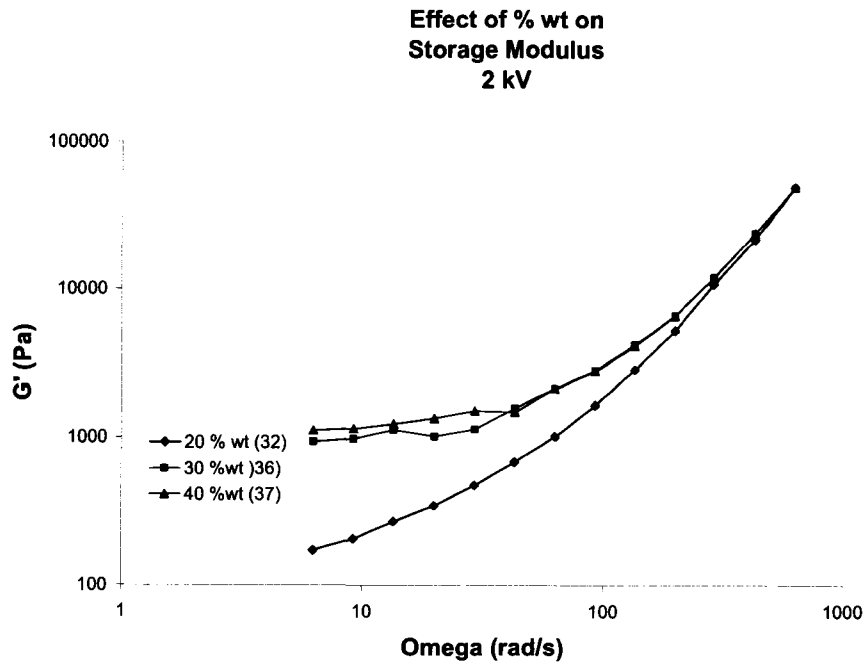
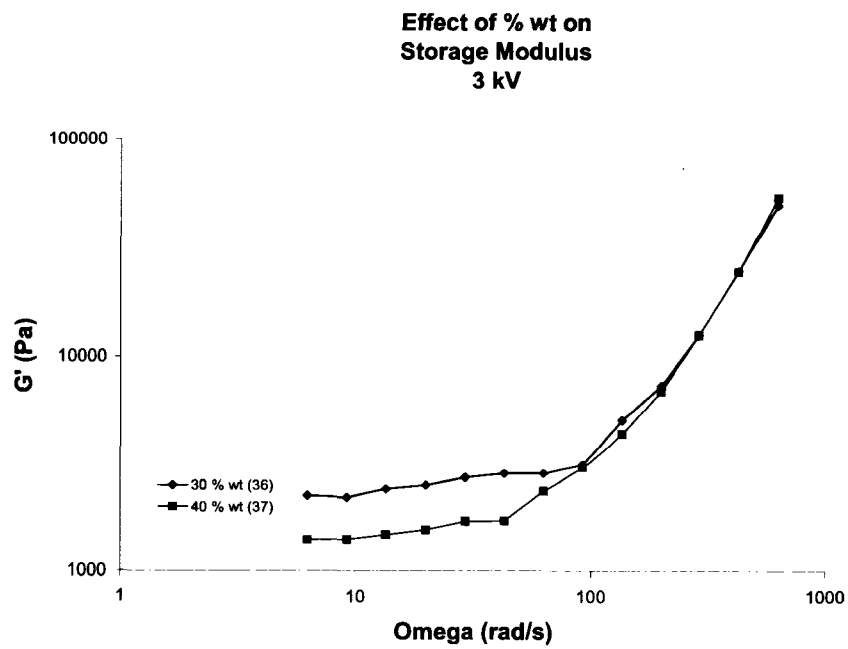


Figure 5.33: G' at 1 kV.

Figure 5.34: G' at 2 kV.Figure 5.35: G' at 3 kV.

REFERENCES

- [1] M.J. Espin, et al, "Optical properties of dilute hematite/silicone oil suspensions under low electric fields," *Journal of Colloid and Interface Science*, 287, pp. 351–359, 2005.
- [2] T. Ó.Thorgeirsdóttir, H.Thormar, T. Kristmundsdóttir, "Viscoelastic properties of a virucidal cream containing the monoglyceride monocaprin: effects of formulation variables," AAPS PharmSciTech.org, Tech. Rep. 7(2): Article 44, DOI: 10.1208/pt070244, 2006.
- [3] T. T. M. Palstra, R. C. Haddon , K. B. Lyons, "Electric current induced light emission from C₆₀," *Carbon*, vol. 35, no.12, pp. 1825-1831, 1997,
- [4] EH&S Manual 6430-T2 Welding Operations, Assessment of and Protection from Welding Arc Radiant Hazards, Thomas Jefferson National Accelerator Facility, 2005.
- [5] Safety and Health Fact Sheet No. 26, Arc Viewing Distance, American Welding Society, 2004
- [6] V.A. Karachevtsev et al, "Effective photopolymerization of C₆₀ films under simultaneous deposition and UV light irradiation: Spectroscopy and morphology study," *Carbon*, vol. 42, no.10, pp. 2091-2098, 2004.
- [7] P. C. Eklund et al, "Optical studies of fullerene-based solids," *Materials Science and Engineering B*, vol. 19, no. 1-2, pp. 154-161, April 1993.

CHAPTER 6

CONCLUSIONS

The scope of this research has shown the electrorheology of C₆₀ suspensions. In this chapter, conclusions and summary of the results are presented. The different weight percents of fullerenes yielded variable results. Samples 31, 36 and 37 showed favorable results over sample 32. This is due to the higher concentrations of the samples.

Fibrillation was visible in samples 32 and 36 with the application of voltage. This suggests that particles are forming chains and columns which are indicative of ER activity. Additionally, particle migration onto the sensor and oscillatory movement of the material inside the sensors was observed in sample 32. A possible explanation for this phenomenon is electrophoretic motion.

Sample 31, 36, and 37 exhibited a positive ER activity. An increase in the storage and loss modulus was observed with increasing voltage. The increase in the elastic behavior of the material was greater than the increase in the viscous behavior. Sample 37 showed a decrease in the storage modulus at voltages greater than 3 kV with increasing values for storage modulus at 0 V when intermittently increasing the voltage. Sample 36 exhibited an increase in storage modulus with the simultaneous application of UV light

and voltage. A photo-ER activity was minimal in sample 37. This may be due to the higher concentration and/or the position and strength UV light.

On occasion, the application of voltage caused a short in the system. The short occurred at either the power source or at the sample site. A short at the power source produced a low audible hissing sound. A short at the sample site produced a loud cracking sound and an emission of a blue to white light. An interesting phenomenon occurred when the short occurred at the sample site. A significant increase in the storage modulus occurred. That increase remained without the application of voltage for an extended period of time. The increase in the storage modulus was not evident when the short occurred at the power source. One of two mechanisms may be responsible for the increase in G' . The first mechanism may be electroluminescence, in which the applied field causes the excited electrons to release energy. The second possible mechanism may be that of an electrical arc in which the UV light emitted by the arc causes the UV sensitive fullerenes to polymerize to some extent, depending on the intensity of the arc.

The microstructure of sample 36_1 was investigated using SEM microscopy. Images revealed formation of numerous fibers with varying lengths, some as large as 60 to 80 microns. It is speculated that the second short that yielded a dominant elastic behavior over the entire frequency range was responsible for the formation of these fibers.

The observations and results of this research project are summarized in Table 6.1. The investigation revealed important and exciting results that may open the doors for

future investigations in C₆₀ fullerenes as ER and photo-ER fluids, as well as, creating carbon fibers under an electric field without high pressures and high temperatures.

Table 6.1: Summary of results and observations.

Sample	% wt C ₆₀	Type	ER Activity	Fibrillation	Particle Migration	Short Site		UV	Fibers
						PS *	Sample		
31	30	Paste	YES	**	**				
32	20	Fluid	NO	X	Yes		X		
36	30	Paste	YES	X	Yes	X	X	X	X
37	40	Paste	YES	**	No	X	X	X	
* PS= power source									
** Indication of non-observance not non-occurrence.									

APPENDIX A

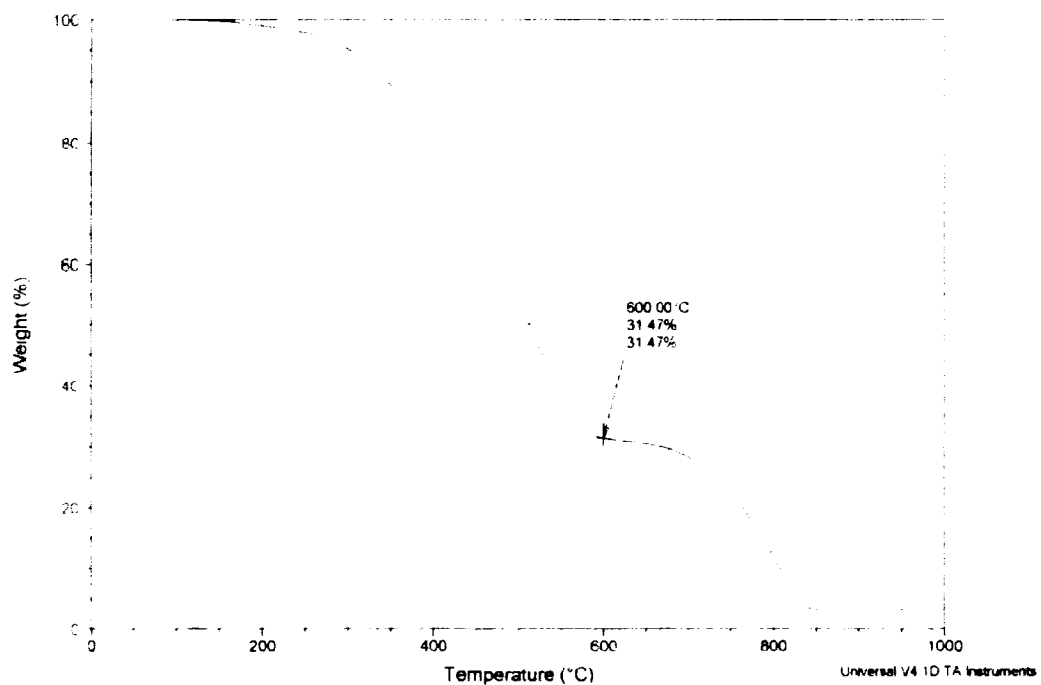
Sample 31

-

Sample: Sample 31
Size: 26.6750 mg
Method: Ramp
Comment: Marcy's Sample 31

TGA

File: C:\TGA\Silicon O\Sample 31 001
Operator: Arturo Alvarez
Run Date: 2006-04-25 13:00
Instrument: TGA Q500 V6.3 Build 189



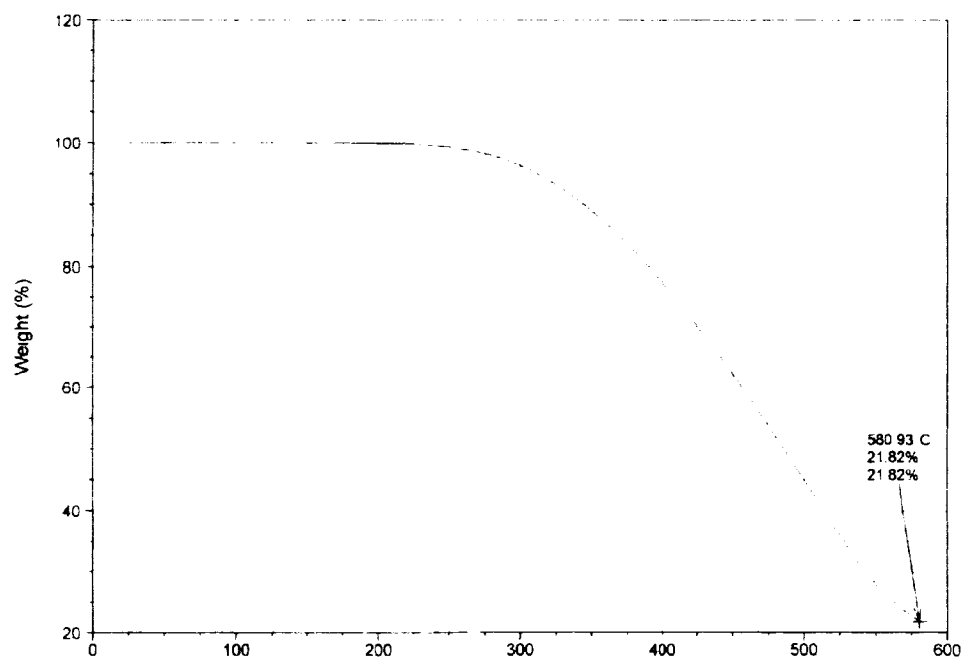
APPENDIX B

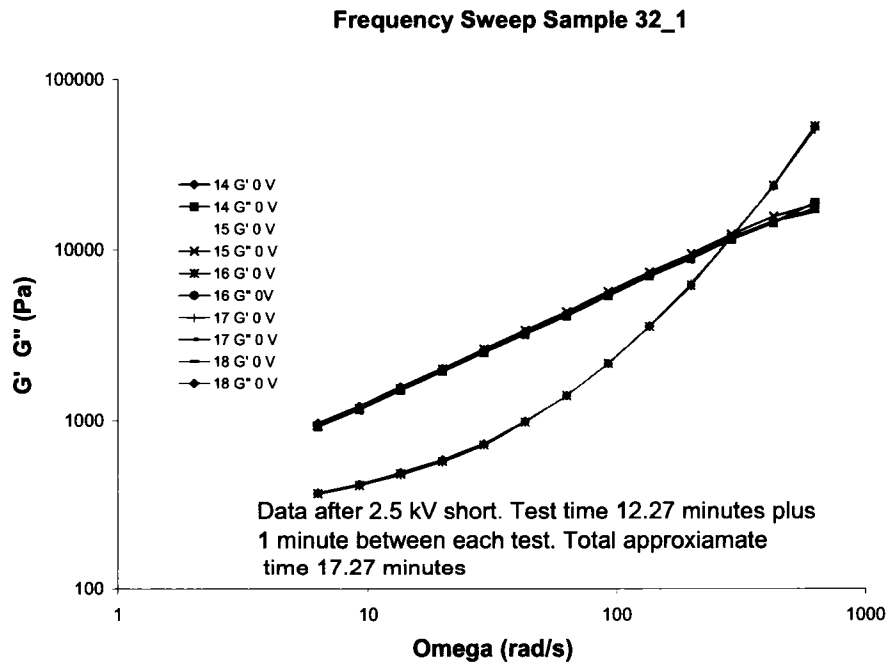
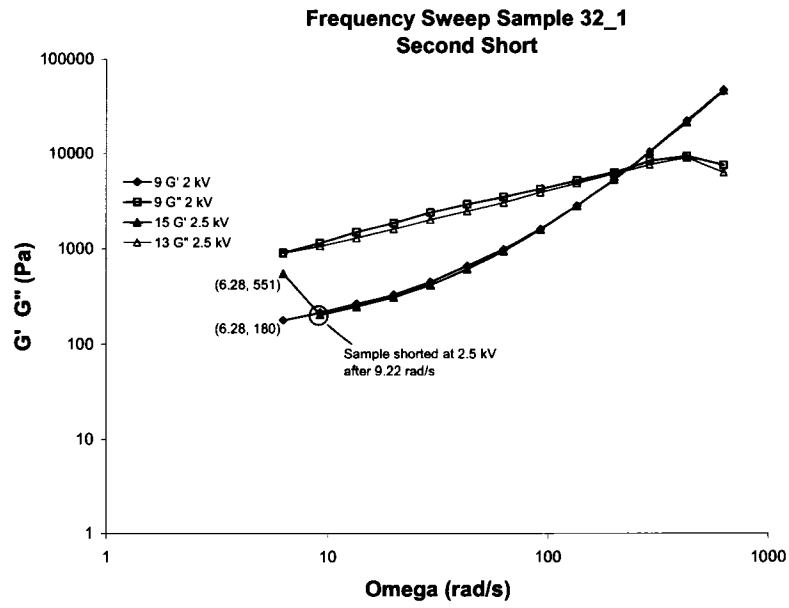
Sample 32

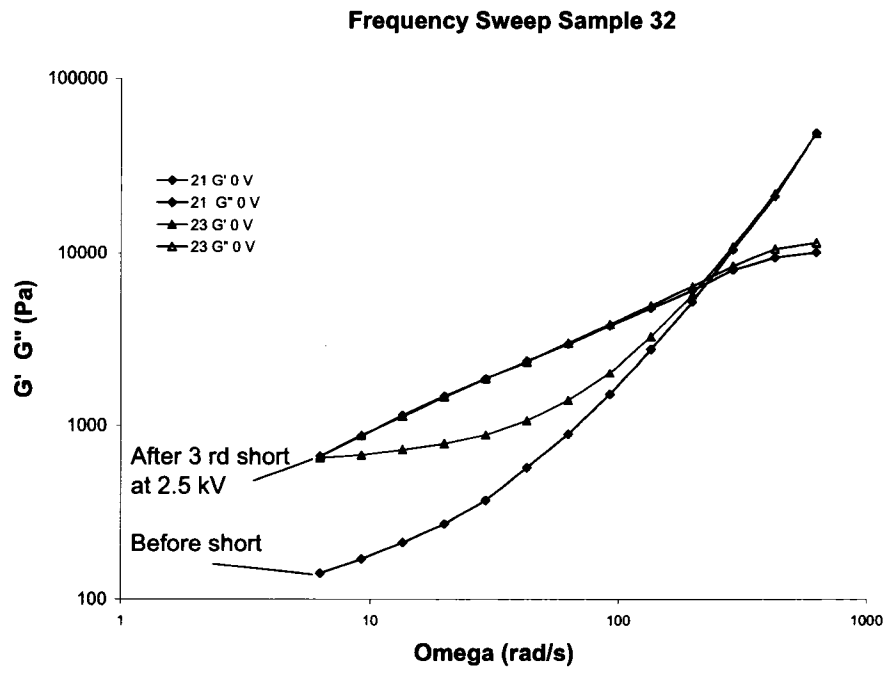
Sample: Sample 32
Size: 22.7700 mg
Method: Ramp
Comment: 20 % Wt Fullerenes 80% Wt: Si Oil

TGA

File: C:\Sample 32 (25C to 600 C) 001
Operator: Arturo Alvarez
Run Date: 2006-07-25 14:28
Instrument: TGA Q500 V6.3 Build 189







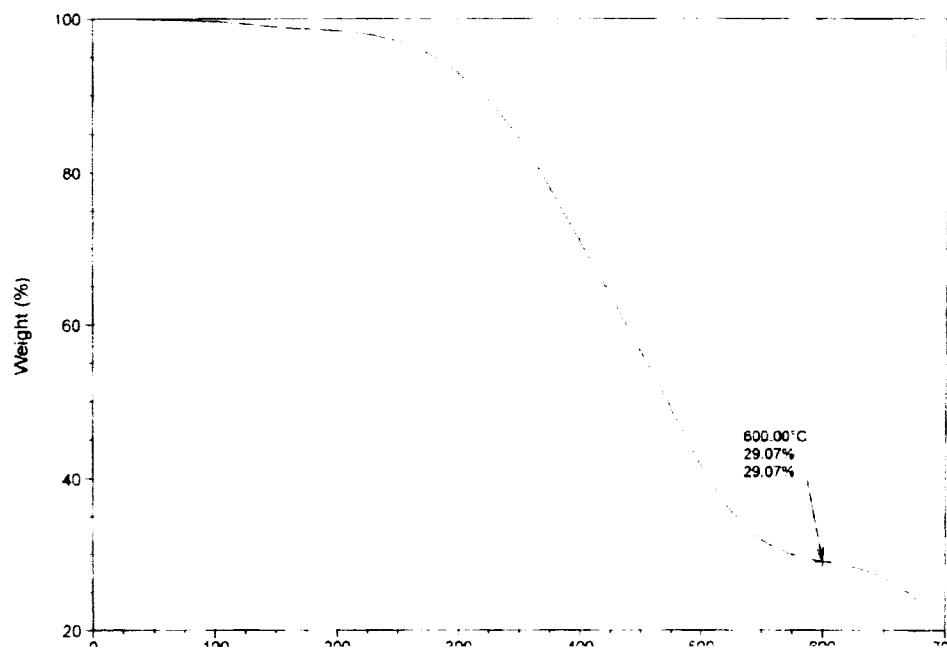
APPENDIX C

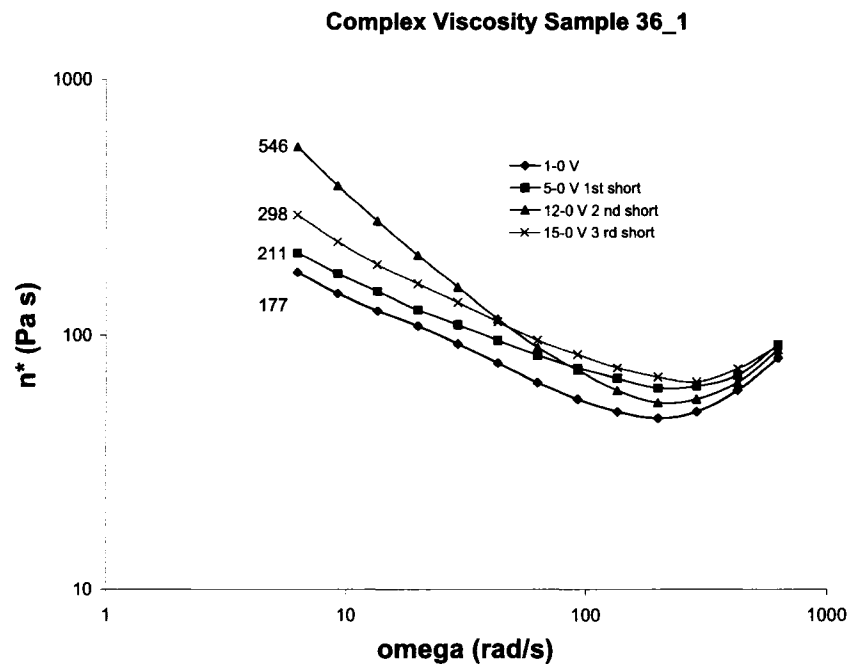
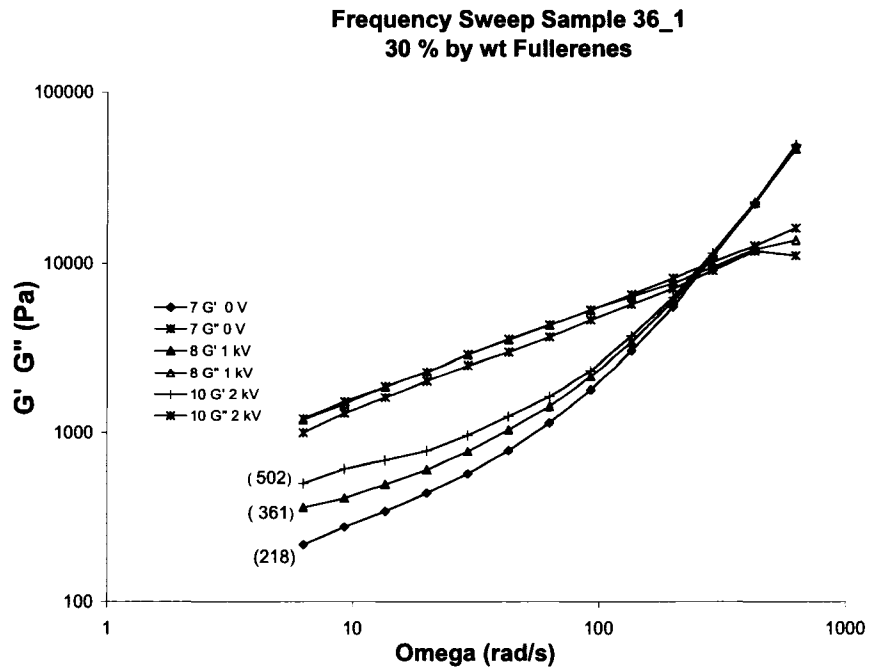
Sample 36

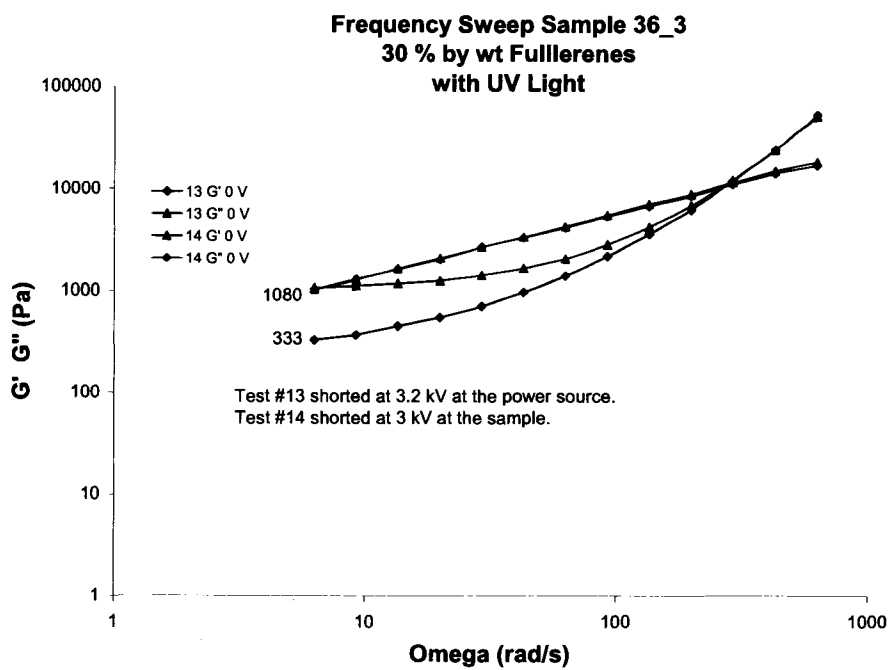
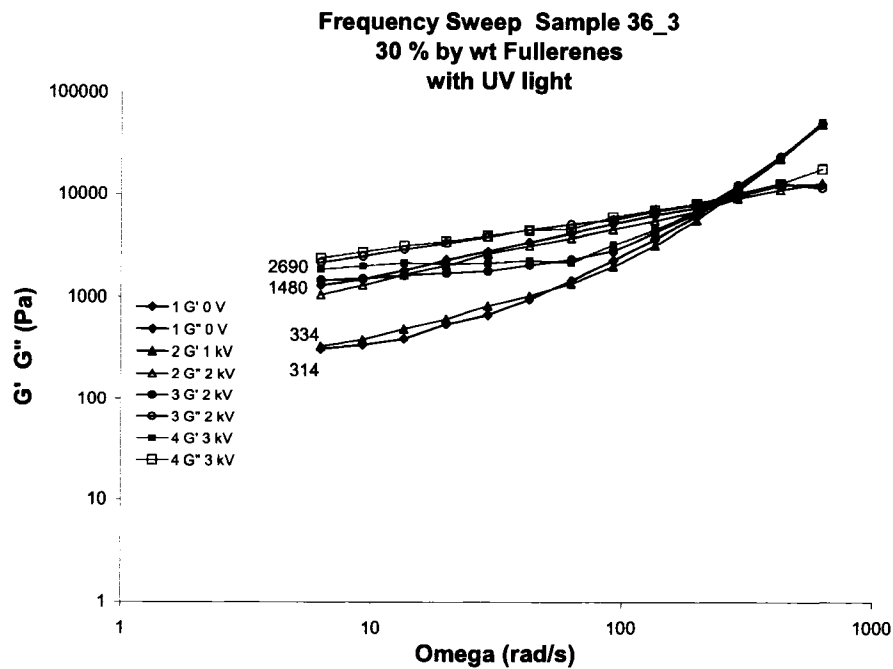
Sample Sample 36
Size 8.0540 mg
Method Ramp
Comment Marcy's Sample 36

TGA

File C:\TGA\Silicon Oil\Sample 36.001
Operator Arturo Alvarez
Run Date 2006-03-17 11:26
Instrument TGA Q500 V6.3 Build 189







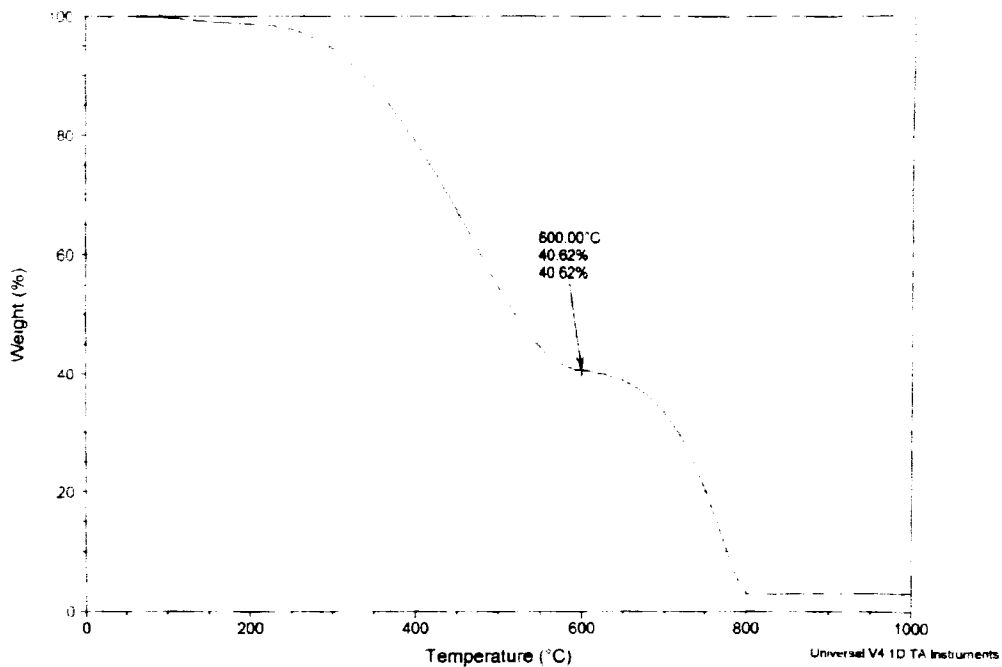
APPENDIX D

Sample 37

Sample Sample 37
Size 8.8790 mg
Method Ramp
Comment Marcy's Sample 37

TGA

File C:\TGA\Siicon On\Sample 37 40
Operator Arturo Alvarez
Run Date 2006-03-21 12:19
Instrument TGA Q500 V6.3 Build 188



VITA

PERSONAL PROFILE

Maricela Lizcano, permanent address: 7410 N. 16th Lane, McAllen, Texas, USA,
born on April 13, 1962 in Waco, Texas, USA.

EDUCATION

Master of Science in Mechanical Engineering from the University of Texas Pan
American, expected date: August 2006; cumulative GPA 3.928.

Bachelor of Science in Mechanical Engineering from the University of Texas Pan
American, May 2004; cumulative GPA 3.404.

EXPERIENCE

2004-2005: HESTEC Robotics Competition Coordinator

2003-2004: HESTEC GE Solar Car Competition Coordinator

2000-2002: Physics Lab Instructor, University of Texas Pan American.

Summer 2004: U. S. Department of Energy, National Renewable Energy Laboratory,
National Wind Technology Center: Boulder, Colorado, USA.

Summer 2001: NSF-REU Vanderbilt University Nashville, Tennessee, USA.

CERTIFICATES

Diploma: Bachelor's Degree in Mechanical Engineering, 2004.

AWARDS

2001 National Collegiate Mathematics Award

2001 NSF-LSAMP Scholarship

2003 Lockheed Martin Scholarship

2004 NSF-LSAMP Bridge to a Doctorate Scholarship

PUBLICATIONS

Mohamamd A. Hannan, Donna Kelly, **Maricela Lizcano**, Giselli Alvarez, "Neutron Activation Analysis of Texas Rio Grande Valley Soils," presented at the Peer-Review Conference Proceeding, 14th Pacific Basin Nuclear Conference, Hawaii, March 20-24, 2004.

APPOINTMENTS

2001: Student member of the Chairman Search Committee for the Department of Physics, University of Texas Pan American

2002: Student member of the Dean Search Committee for the College of Science and Engineering, University of Texas Pan American

PRESENTATIONS

Feb. 2001: South Texas Mathematics Conference, University of Texas, Brownsville, TX.

Mar. 2001: Texas Section Mathematics Association, University of Houston, Houston, TX.

ORGANIZATIONS

Phi Kappa Phi Honor Society, the American Society for Engineering Education, Society of Women Engineers, Society of Hispanic Professional Engineers, American Society of Mechanical Engineers.